Available online at www.sciencedirect.com

ScienceDirect

Geochimica et Cosmochimica Acta 165 (2015) 226–248

Geochimica et Cosmochimica Acta

www.elsevier.com/locate/gca

Dissolved inorganic carbon (DIC) and its $\delta^{13}C$ in the Ganga (Hooghly) River estuary, India: Evidence of DIC generation via organic carbon degradation and carbonate dissolution

Saumik Samanta [a,*], Tarun K. Dalai [a,*], Jitendra K. Pattanaik [a], Santosh K. Rai [b], Aninda Mazumdar [c]

[a] *Indian Institute of Science Education and Research Kolkata, Mohanpur 741246, India*
[b] *Wadia Institute of Himalayan Geology, Dehradun 248001, India*
[c] *National Institute of Oceanography, Donapaula 403004, India*

Received 20 December 2014; accepted in revised form 26 May 2015; available online 1 June 2015

Abstract

In this study, we present comprehensive data on dissolved Ca, dissolved inorganic carbon (DIC) and its carbon isotope composition ($\delta^{13}C_{DIC}$) of (i) the Ganga (Hooghly) River estuary water sampled during six seasons of contrasting water discharge over 2 years (2012 and 2013), (ii) shallow groundwater from areas adjacent to the estuary and (iii) industrial effluent water and urban wastewater draining into the estuary. Mass balance calculations indicate that processes other than the conservative mixing of seawater and river water are needed to explain the measured DIC and $\delta^{13}C_{DIC}$. Results of mixing calculations in conjunction with the estimated undersaturated levels of dissolved O_2 suggest that biological respiration and organic carbon degradation dominate over biological production in the estuary. An important outcome of this study is that a significant amount of DIC and dissolved Ca is produced within the estuary at salinity $\geqslant 10$, particularly during the monsoon period. Based on consideration of mass balance and a strong positive correlation observed between the "excess" DIC and "excess" Ca, we contend that the dominant source of DIC generated within the estuary is carbonate dissolution that is inferred to be operating in conjunction with degradation of organic carbon. Calculations show that groundwater cannot account for the observed "excess" Ca in the high salinity zone. Estimated DIC contributions from anthropogenic activity are minor, and they constitute ca. 2–3% of the river water DIC concentrations.

The estimated annual DIC flux from the estuary to the Bay of Bengal is ca. (3–4) $\times 10^{12}$ g, of which ca. 40–50% is generated within the estuary. The monsoon periods account for the majority (ca. 70%) of the annual DIC generation in the estuary. The annual DIC flux from the Hooghly estuary accounts for ca. 1% of the global river DIC flux to the oceans. This is disproportionately higher than the water contribution from the Hooghly River to the oceans, which accounts for ca. 0.2% of the global river water flux. The results of this study suggest that estuaries in regions affected by tropical monsoon can be important in terms of their production of significant amounts of DIC and its delivery to the world's oceans.

1. INTRODUCTION

Understanding carbon cycling and exchange of CO_2 in various reservoirs with the atmosphere is important in light

* Corresponding authors.
E-mail addresses: saumik1215@iiserkol.ac.in, saumik.papan@gmail.com (S. Samanta), dalai@iiserkol.ac.in, dalaitk@gmail.com (T.K. Dalai).

http://dx.doi.org/10.1016/j.gca.2015.05.040
0016-7037/

of the continuous increase in atmospheric CO_2 concentration in recent times (Keeling et al., 1979, 1980; Hunt et al., 1996; Fearnside, 2000). Rivers and estuaries act as the major pathways for transport of terrestrial carbon to the oceans and the atmosphere (Schulte et al., 2011, and references therein). The annual riverine dissolved inorganic carbon (DIC) flux to the oceans is estimated at ca. 0.4 Gt (Meybeck, 1993; Bauer et al., 2013) compared to the combined dissolved and particulate carbon flux of ca. 0.8–1.0 Gt (Amiotte Suchet et al., 2003; Cole et al., 2007; Battin et al., 2009; Bauer et al., 2013; Regnier et al., 2013). These fluxes are vastly influenced by several estuarine processes because carbon participates in a number of organic and inorganic processes such as biological productivity, oxidation/degradation of organic carbon, dissolution and precipitation of calcite and exchange of CO_2 with the atmosphere. For instance, recent studies show that significant outgassing of riverine carbon to the atmosphere is driven by the high pCO_2 of river waters compared to that of the atmosphere (Richey et al., 2002; Zhai et al., 2005; Yao et al., 2007; Dubois et al., 2010; van Geldern et al., 2015).

The Ganga River system is the largest river system in India in terms of water and sediment discharge (Milliman and Meade, 1983). The Ganga River splits into two branches at Farakka; one branch flows through India and is called the Hooghly River; the other enters Bangladesh and is called the Padma River. The Hooghly River passes through the densely populated city of Kolkata and acts as a navigable waterway. In addition, the estuary water receives effluent from several industries located in the vicinity of Haldia and Diamond Harbour. Thus, the estuary receives and transforms products of both natural and anthropogenic origin that are likely to affect biogeochemical processes, and influence concentrations and distribution of nutrients, elements and their isotopes. A number of studies have been conducted that investigate chemical weathering in the Ganga River basin based on major ions, trace elements and isotope chemistry of waters and sediments of the Ganga River and its tributaries in the upper and lower reaches (Sarin et al., 1989; Singh et al., 1998, 2008; Dalai et al., 2002a,b,c; Rai et al., 2010). However, a detailed study of carbon cycling and its influence on the abundance and distribution of DIC in the Ganga (Hooghly) River estuary is lacking.

Stable isotope compositions of dissolved inorganic carbon (DIC) have been used as a powerful tool to understand the sources and cycling of carbon in rivers and estuaries (Hélie et al., 2002; Brunet et al., 2005; Ahad et al., 2008; Doctor et al., 2008; Schulte et al., 2011). In this study, we provide a comprehensive dataset on the abundance and distribution of DIC, carbon isotope composition of DIC ($\delta^{13}C_{DIC}$) and particulate organic carbon ($\delta^{13}C_{POC}$) in the Hooghly River estuary along the salinity transition zone. In addition, we also present data on DIC concentrations and $\delta^{13}C_{DIC}$ of shallow groundwater collected from areas adjacent to the estuary, and for industrial effluent and urban wastewater draining into the estuary. Considering that the Hooghly River estuary is mainly heterotrophic (Mukhopadhyay et al., 2002) despite being a site of significant and seasonally variable primary productivity, degradation and respiration of organic carbon are expected to contribute DIC to the estuary. One of the primary goals of this study is to determine the significance of this process, and to understand other important sources and sinks of DIC. This study also attempts to assess how significantly anthropogenic activities impact the carbon cycling in the Hooghly River estuary. Based on the data and calculations, we have addressed the role of several processes that contribute to variation in DIC and $\delta^{13}C_{DIC}$, and have shown that cycling of both organic and inorganic carbon are closely linked in the Hooghly River estuary. The data and information of this study on the cycling and transport of carbon in an important tropical monsoon river system of the world are valuable in that they can be used in modelling of the global carbon cycle.

2. THE STUDY AREA

The Ganga River originates near the Gangotri glacier, located in the Garhwal region of the western Himalayas. The mainstream of the Ganga is formed at Devaprayag, where it has an average water discharge of ~700 m^3/s (AHEC, 2011). As it descends to the alluvial plain, the Ganga River is fed by several tributaries draining the Himalayas. After flowing for more than 2000 km from its origin, the Ganga River bifurcates near Farakka (Fig. 1). The main distributary of the Ganga, the Hooghly River, flows southwards and drains into the Bay of Bengal (Fig. 1). The depth of the estuary varies along the channel from 21 m (~70 ft) at Diamond Harbour (Fig. 2) to ~8 m (25 ft) at the mouth of the estuary (CIFRI, 2012). The Hooghly main channel is much deeper than its distributary, the Muriganga channel (~6 m; Sadhuram et al., 2005).The width of the river at the mouth of the estuary is ~25 km (Mukhopadhyay et al., 2006). Annual rainfall over the last 5 years (2009–2013) in and around the Hooghly River estuary varied from ~1310 mm to ~2300 mm (IMD, 2013). Approximately 80% of the annual rainfall occurs during the southwest monsoon (June–September). Upstream of Farakka, the average water discharge of the Ganga River is ~14,527 m^3/s water (AHEC, 2011), which is ~1.2% of the world's river water flow. From the Farakka Barrage, which was constructed to control the Ganga water flow, fresh water discharge to the Hooghly River varies from 900 m^3/s in the dry season to 4000 m^3/s in the monsoon season (Mukhopadhyay et al., 2006). The discharge of the Hooghly River is increased by additional input of water from tributaries such as the Rupnarayan and the Damodar rivers. The Hooghly River carries 328×10^{12} g of suspended sediment annually (Abbas and Subramanian, 1984). The Hooghly estuary receives approximately 13 m^3/s of industrial effluent and urban wastewater (Sadhuram et al., 2005, and references therein) from densely populated and industrial cities such as Kolkata, Haldia and Howrah (Fig. 2). In addition, the Hooghly estuary is extensively used as the navigable waterway for two major ports (Kolkata and Haldia) and the Sunderban islands. The Sunderbans, the largest mangrove forest in the world, is located in the eastern margin of the Hooghly estuary

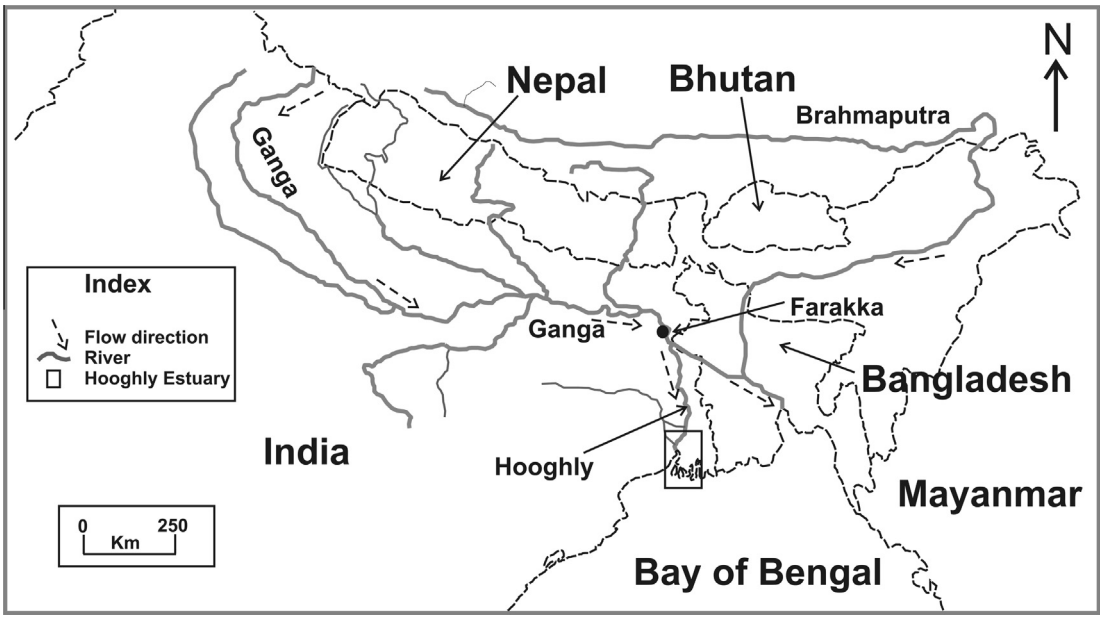

Fig. 1. Map of the Ganga–Brahmaputra river system. Downstream of Farakka, the Ganga River splits into two channels: the Hooghly River flows through India, and the Padma River flows through Bangladesh.

(Fig. 2) and may contribute to the nutrient budget of the lower reaches of the estuary.

3. SAMPLING AND METHODOLOGY

3.1. Sample collection

Collection of dissolved, suspended and bed load samples was carried out over 2 years (2012–2013) during pre-monsoon (April–May), monsoon (July–August) and post-monsoon (October–November) periods. The samples were collected along the longitudinal transect mostly from the main channel of the Hooghly estuary (Fig. 2). A few samples of industrial effluent and wastewaters from the cities of Kolkata and Haldia that drain into the main Hooghly channel were also collected (Fig. 2, Table 1). In most cases, water sampling was carried out from the middle of the channel either using a boat or from platforms (jetties) constructed along the banks of the river. All water samples were collected from the surface of the flowing water. A few groundwater samples were collected from locations that are close to the river. The depth of the groundwater samples varied from ~15 to 76 m (Table 1). For analysis of major cations and trace elements, approximately 250 ml of samples were filtered through 0.4 μm Nucleopore® polycarbonate filters within 12 h of sampling. Only a few samples were filtered within 24 h of collection. Aliquots of the filtered samples were acidified to pH < 2 using ultrapure nitric acid (Tamapure®) and stored in pre-cleaned HDPE bottles. For $\delta^{13}C$ analysis, samples were collected in 30 ml amber bottles after filtering waters in the field through 0.45 μm PTFE syringe filters, and were immediately poisoned by adding saturated $HgCl_2$ (10 μl in ~30 ml sample). In addition, 30 ml samples were collected separately for measurement of carbonate alkalinity. Suspended sediments were collected after decanting ca. 5 l of river/estuary water and then centrifuging the residues at 5000 rpm. These sediments were dried at 70 °C and powdered to <100 mesh size using an agate pestle-mortar assembly.

3.2. Analyses

Salinity, pH and temperature were measured *in situ* using portable multi-electrode probes (Eutech PCSTestr 35and Hach HQ40d). Measurement accuracies were ±0.05 for pH and ±0.01 for salinity. Dissolved oxygen (DO) was measured *in situ* using a portable field probe (Hach HQ40d-LDO). Total carbonate alkalinity (CO_3^{2-} and HCO_3^-) was measured within 24 h of sample collection by both routine indicator-based acid-base titration and potentiometric titration using an auto-titrator (Metrohm 916 Ti-touch). The sum of bicarbonate and carbonate alkalinity is hereafter referred to as dissolved inorganic carbon (DIC). Based on repeated analyses of a Merck® sodium bicarbonate standard, the accuracy of DIC measurement was ascertained to be ca. 0.5% ($n = 6$) and 0.25% ($n = 5$), respectively, for indicator-based and auto-titrator analyses. Average agreement between DIC concentrations for duplicate analyses was 0.85 ± 0.52% (1 SD, $n = 12$). Dissolved Ca was measured by ion chromatography (Themoscientific Dionex ICS-5000). Based on analyses of reference standard BCR-617, accuracy of Ca measurement is better than 3%. Average reproducibility of Ca concentrations is ca. 1.2 ± 0.5% (1 SD, $n = 14$) based on repeat analyses of samples.

$\delta^{13}C_{DIC}$ measurements were carried out at Wadia Institute of Himalayan Geology (WIHG), Dehradun. Approximately 700 μl of filtered water was injected into a septum-closed vial (10 ml Labco vial) flushed with helium and containing phosphoric acid (50–70 μl of >99% purity

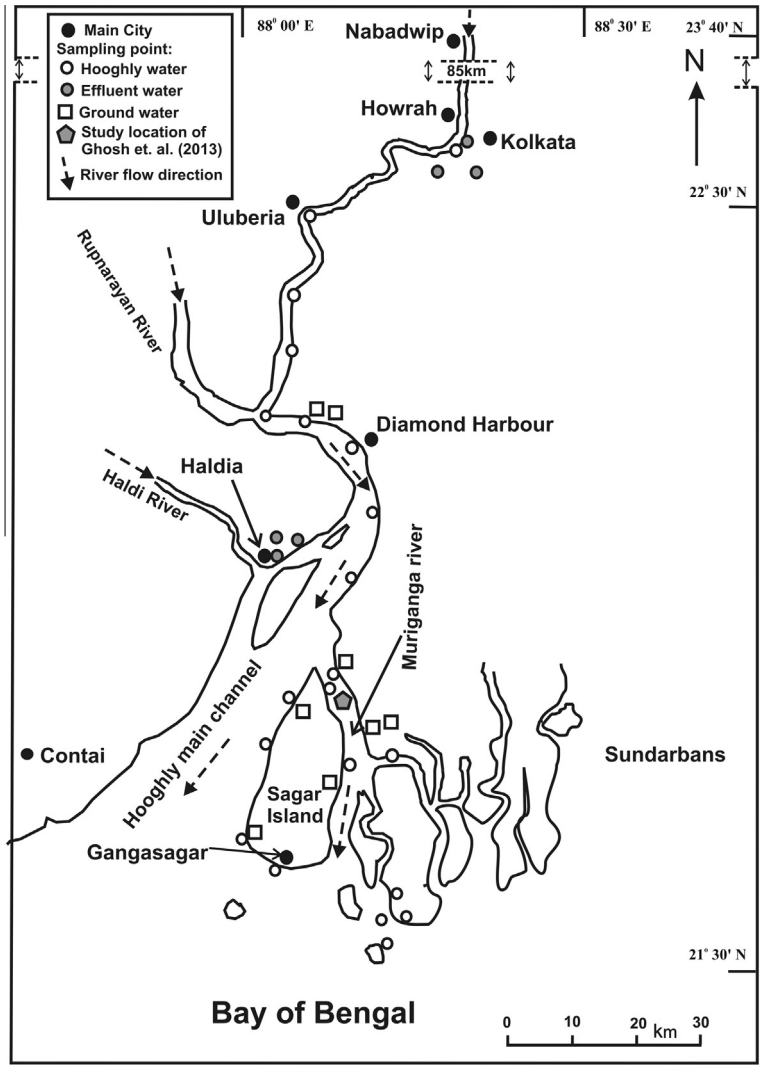

Fig. 2. Map showing the sampling locations for the Hooghly water, shallow groundwater and effluent water. The sampling point of Ghosh et al. (2013) in the Muriganga channel is also shown.

H_3PO_4). The samples were kept in the vial for eighteen hours to ensure that all DIC is converted to gaseous CO_2 and to ensure complete equilibration between the two phases. After removal of the moisture and purification, CO_2 gas purged from the sample was introduced into a Continuous Flow Isotope Ratio Mass Spectrometer (CF-IRMS; Thermo-Finnigan Delta V Plus). Accuracy was better than 0.2‰ based on repeated analyses of a laboratory standard (Merck® $CaCO_3$) that was calibrated against reference standard NBS-18. Average instrumental precision was ca. 0.1‰ for the samples and standards analyzed. The $\delta^{13}C_{POC}$ of suspended sediments was analyzed at the National Institute of Oceanography (NIO), Goa. Approximately 8 mg of decarbonated sample was packed in a tin capsule and combusted in the reactor. The CO_2 liberated was introduced into a continuous flow isotope ratio mass spectrometer (CF-IRMS; Thermo-Finnigan Delta V Plus) attached to an elemental analyzer (Thermo EA1112). The IAEA Cellulose C3 standard was analyzed during the course of the analysis and yielded a $\delta^{13}C$ value of -24.75 ± 0.07‰ VPDB (1 SD). This result is in good agreement with the certified value of -24.91 ± 0.49‰. The precision of $\delta^{13}C_{POC}$ measurements is 0.07‰ based on repeated analyses of the standards.

4. RESULTS

The salinity of the Hooghly estuary samples varied from 0.16–25.92 during pre-monsoon, 0.12–18.84 during monsoon and 0.12–14.46 during post-monsoon seasons (Table 1). The temperature of water samples varied from 24 to 35 °C, and the pH ranged from 7.2 to 8.5. Dissolved Ca concentrations were in the range from 0.58 to 9.18 mM for all Hooghly samples, and they varied from 0.58 to 0.94 mM in fresh waters ($S \leqslant 0.3$). The DIC concentrations varied from 1.68 to 2.67 mM for all samples collected over 2 years (Table 1, Fig. 3). Freshwaters of the Hooghly River have higher concentrations of DIC

Table 1
Location details, chemical and carbon isotope composition ($\delta^{13}C_{DIC}$) of Hooghly water, groundwater and effluent water.

Sample code	Date	Location	Latitude (N)	Longitude (E)	Temperature (°C)	pH	Salinity	DIC (mM)	$\delta^{13}C_{DIC}$ (‰ VPDB)	DO[#] (mM)	Ca (mM)
Hooghly											
HGH12–13	22.05.2012	Princep Ghat	22°33′ 21″	88°19′ 50″	32.0	8.31	0.16	2.52	−5.7	NM	0.83
HGH12–12	22.05.2012	Achhipur	22°27′ 36″	88°07′ 21″	33.8	8.26	0.16	2.54	−5.6	NM	0.83
HGH12–11	22.05.2012	Burul	22°21′ 46″	88°06′ 17″	32.0	8.15	0.21	2.58	−5.7	NM	0.77
HGH12–5	21.05.2012	Falta	22°17′ 27″	88°06′ 13″	31.6	8.50	0.60	2.61	−5.6	NM	0.82
HGH12–6	21.05.2012	Raychalk	22°12′ 28″	88°07′ 15″	34.0	8.35	1.02	2.59	−5.6	NM	1.05
HGH12–1	12.05.2012	Diamond Harbour[H]	22°11′ 05″	88°11′ 22″	30.3	8.09	2.50	2.48	−5.1	NM	1.61
HGH12–1A	22.05.2012	Diamond Harbour[L]	22°11′ 06″	88°11′ 22″	31.3	8.45	1.12	2.67	−4.4	NM	0.82
HGH12–2	12.05.2012	Kulpi	22°05′ 01″	88°13′ 19″	31.4	8.32	3.44	2.50	−5.1	NM	1.92
HGH12–3	12.05.2012	Kakdwip Lot No. 8	21°52′ 51″	88°09′ 53″	30.6	8.28	15.87	2.32	NM	NM	5.77
HGH12–7	21.05.2012	Kachuberia Ghat	21°51′ 33″	88°08′ 41″	34.3	8.16	16.52	2.36	−4.4	NM	6.19
HGH12–8	21.05.2012	Sapkhali	21°50′ 44″	88°06′ 45″	33.2	8.04	14.84	2.48	−3.9	NM	5.47
HGH12–9	21.05.2012	Light House	21°39′ 26″	88°02′ 29″	31.3	8.15	24.48	2.29	−3.6	NM	9.18
HGH12–10	21.05.2012	Gangasagar	21°37′ 53″	88°04′ 24″	31.5	8.15	25.92	2.32	−2.3	NM	9.16
HGH12–4	12.05.2012	Namkhana	21°45′ 41″	88°14′ 06″	30.3	8.25	21.16	2.25	−2.3	NM	7.58
HGH12–26	14.07.2012	Achhipur	22°27′ 36″	88°07′ 21″	30.7	8.04	0.12	1.85	−7.0	NM	0.68
HGH12–25	14.07.2012	Burul	22°21′ 46″	88°06′ 17″	30.6	7.96	0.12	1.83	−7.1	NM	0.68
HGH12–24	14.07.2012	Falta	22°17′ 27″	88°06′ 14″	31.5	7.92	0.12	1.86	−7.1	NM	0.67
HGH12–23	14.07.2012	Raychalk	22°12′ 28″	88°07′ 15″	31.6	8.09	0.29	1.73	−7.0	NM	0.69
HGH12–22	14.07.2012	Diamond Harbour	22°11′ 06″	88°11′ 22″	31.1	8.01	0.65	1.76	−6.1	NM	0.79
HGH12–21	14.07.2012	Kulpi	22°05′ 02″	88°13′19″	31.9	8.12	0.81	1.68	−8.1	NM	0.88
HGH12–19	13.07.2012	Kakdwip Lot No. 8	21°52′51″	88°09′53″	31.0	8.03	11.00	2.10	−4.8	NM	4.56
HGH12–14	13.07.2012	Kachuberia Ghat	21°51′33″	88°08′41″	30.6	8.18	11.28	2.11	−4.8	NM	4.73
HGH12–15	13.07.2012	Sapkhali	21°51′02″	88°06′52″	32.8	7.83	9.15	2.06	−4.6	NM	3.91
HGH12–18	13.07.2012	Mandirtala	21°46′53″	88°04′36″	35.0	8.08	15.27	2.20	−4.4	NM	5.89
HGH12–16	13.07.2012	Light House	21°39′26″	88°02′29″	31.7	8.07	17.55	2.20	−4.0	NM	6.58
HGH12–17	13.07.2012	Gangasagar	21°37′53″	88°04′24″	32.0	8.03	18.84	2.19	−3.8	NM	7.00
HGH12–20	13.07.2012	Namkhana	21°45′41″	88°14′06″	30.4	8.00	18.54	2.24	−3.6	NM	6.99
HGH12–40	05.10.2012	Burul	22°21′46″	88°06′17″	30.5	7.65	0.12	2.25	−10.2	NM	0.78
HGH12–39	05.10.2012	Nurpur	22°12′42″	88°04′17″	30.7	7.59	0.16	2.21	−11.4	NM	0.69
HGH12–35	05.10.2012	Diamond Harbour[L]	22°11′06″	88°11′22″	29.8	7.43	0.23	2.17	−11.0	NM	0.66
HGH12–38	05.10.2012	Diamond Harbour[H]	22°11′06″	88°11′22″	30.7	7.61	0.20	2.11	−10.0	NM	0.70
HGH12–36	05.10.2012	Kulpi	22°05′02″	88°13′19″	30.3	7.86	0.30	2.10	−11.1	NM	0.70
HGH12–37	05.10.2012	Nischindipur	21°59′47″	88°11′25″	30.6	7.69	0.43	2.05	−10.3	NM	0.69
HGH12–31	03.10.2012	Kachuberia Ghat	21°51′33″	88°08′41″	29.8	7.67	2.56	2.03	−9.7	NM	1.35
HGH12–30	03.10.2012	Sapkhali	21°49′16″	88°05′52″	29.7	7.78	4.23	2.07	−9.2	NM	1.89
HGH12–29	03.10.2012	Mandirtala	21°46′53″	88°04′36″	29.2	7.93	5.08	2.07	−9.6	NM	2.36
HGH12–28	03.10.2012	Light House	21°39′26″	88°02′29″	29.2	7.88	10.83	1.89	−8.6	NM	4.10
HGH12–27	03.10.2012	Gangasagar	21°37′53″	88°04′24″	29.4	7.89	10.5	1.95	−10.1	NM	4.10
HGH12–32	04.10.2012	Namkhana	21°45′41″	88°14′06″	30.4	7.59	7.95	2.01	−9.4	NM	3.17
HGH12–33	04.10.2012	Freserganj	21°34′34″	88°14′54″	29.4	7.69	13.2	1.82	−7.9	NM	4.79
HGH12–34	04.10.2012	Bakkhali	21°33′51″	88°14′52″	29.4	7.72	13.5	1.99	−7.9	NM	4.92
HGH13–12	25.04.2013	Acchipur	22°27′36″	88°07′21″	31.9	7.99	0.19	2.35	−4.0	0.217	0.94
HGH13–11	25.04.2013	Burul	22°21′46″	88°06′17″	30.5	8.14	0.65	2.26	−4.1	0.218	1.11

HGH13–10	25.04.2013	Raychalk	22°12′28″	88°07′15″	30.0	8.26	1.32	2.19	−4.0	0.223	1.35
HGH13–1	23.04.2013	Diamond Harbour	22°11′06″	88°11′22″	29.3	8.08	2.04	2.24	−3.2	0.207[DP]	1.32
HGH13–2	23.04.2013	Kulpi	22°05′02″	88°13′19″	33.0	8.16	2.71	2.41	−4.7	0.216	1.56
HGH13–3	23.04.2013	Nischindipur	21°9′47″	88°11′25″	29.0	8.21	6.82	2.24	−4.3	0.223	2.86
HGH13–4	23.04.2013	Kakdwip Lot No. 8	21°52′51″	88°09′53″	31.0	8.06	13.38	2.12	−4.9	0.232	4.39
HGH13–9	24.04.2013	Kachuberia ghat	21°51′33″	88°08′40″	29.1	8.01	12.3	2.08	−3.7	0.225	4.43
HGH13–8	24.04.2013	Sapkhali	21°49′16″	88°05′52″	31.0	8.03	17.37	2.13	−2.8	0.233	6.35
HGH13–7	24.04.2013	Light House	21°39′26″	88°02′29″	31.3	8.14	25.2	1.87	−2.2	0.227	7.78
HGH13–6	24.04.2013	Gangasagar	21°37′53″	88°04′24″	31.5	8.11	25.88	1.90	−1.6	0.227	7.97
HGH13–5	23.04.2013	Namkhana	21°45′41″	88°14′06″	30.0	8.06	17.76	2.05	−3.0	0.219	5.91
HGH13–14	10.08.2013	Falta	22°17′27″	88°06′14″	29.7	7.55	0.20	1.93	−3.6	0.208	0.70
HGH13–15	10.08.2013	Diamond Harbour	22°11′06″	88°11′22″	30.5	7.69	0.17	1.95	−3.2	0.190[DP]	0.71
HGH13–16	10.08.2013	Kulpi	22°05′02″	88°13′19″	30.3	7.71	0.29	1.91	−4.0	0.212	0.66
HGH13–17	10.08.2013	Nischindipur	21°59′47″	88°11′25″	30.8	7.66	1.00	1.97	−5.8	0.208	0.88
HGH13–18	10.08.2013	Kakdwip Lot No. 8.[L]	21°52′51″	88°09′53″	30.4	7.67	6.31	2.00	−4.9	0.216	2.52
HGH13–20	11.08.2013	Kakdwip Lot No. 8.[M]	21°52′51″	88°09′53″	31.0	7.85	3.58	2.09	−5.4	0.226	1.70
HGH13–21	11.08.2013	Kakdwip Lot No. 8.[H]	21°52′51″	88°09′53″	28.5	7.70	5.11	2.07	−4.4	0.223	2.28
HGH13–22	11.08.2013	Freserganj	21°34′34″	88°14′54″	29.0	8.02	14.31	2.16	−3.3	0.220	5.28
HGH13–23	11.08.2013	Freserjanj Mohana	21°34′50″	88°14′01″	28.2	7.77	12.75	2.23	−4.0	0.222	4.81
HGH13–24	11.08.2013	Near Jammu Dwip	21°32′06″	88°13′07″	28.6	8.05	15.06	2.14	−2.6	0.219[DP]	5.49
HGH13–19	10.08.2013	Namkhana	21°45′41″	88°14′06″	30.0	7.78	9.32	2.15	−4.3	0.217	3.76
HGH13–25	15.11.2013	Diamond Harbour	22°11′06″	88°11′22″	25.0	7.21	0.15	2.16	−6.6	0.215	0.58
HGH13–26	15.11.2013	Kulpi	22°05′02″	88°13′19″	25.6	7.59	0.18	2.13	−6.1	0.244	0.58
HGH13–27	15.11.2013	Nischindipur	21°59′48″	88°11′25″	27.1	7.69	0.29	2.00	−6.9	0.231	0.63
HGH13–28	15.11.2013	Kakdwip Lot No. 8[L]	21°52′51″	88°09′53″	27.0	7.63	2.32	1.87	−7.0	0.232	1.28
HGH13–35	16.11.2013	Kakdwip Lot No. 8[L]	21°52′54″	88°09′53″	24.8	7.75	2.23	1.89	−7.5	0.233	1.26
HGH13–34	16.11.2013	Kachuberia ghat	21°51′34″	88°08′41″	24.8	7.8	1.16	1.92	−7.5	0.238	0.86
HGH13–31	16.11.2013	Muriganga	21°49′12″	88°09′42″	26.1	7.82	6.15	1.81	−6.7	0.249	2.65
HGH13–33	16.11.2013	Light House	21°39′26″	88°02′29″	27.0	7.83	8.80	1.87	−5.6	0.248	3.57
HGH13–32	16.11.2013	Gangasagar	21°37′53″	880 04′24″	26.7	7.94	11.74	1.79	−4.9	0.247	4.59
HGH13–29	15.11.2013	Namkhana	21°45′41″	88°14′06″	28.5	7.70	5.30	1.79	−6.5	0.234	2.30
HGH13–30	15.11.2013	Bakkhali	21°33′51″	88°14′52″	26.1	7.80	14.46	1.70	−4.0	0.246	5.45
Tributary											
HGH13/T-1	25.04.2013	Bethobati Khal	22°27′27″	88°07′14″	31.3	8.10	0.19	2.31	NM	0.131	0.90
Groundwater											
HGH13/SGW-1	23.04.2013	Kakdwip (61 m)	21°52′44″	88°10′03″	30.2	7.85	0.53	4.80	−6.7	0.088	0.75
HGH13/SGW-2	24.04.2013	Sapkhali (67 m)	21°50′39″	88°06′42″	31.2	8.22	0.46	5.16	−7.4	0.072	0.58
HGH13/SGW-3	25.04.2013	Raychalk (46 m)	22°12′37″	88°07′30″	28.0	7.09	4.21	11.21	−13.3	0.198	6.49
HGH13/SGW-4	25.04.2013	Raychalk (34 m)	22°13′14″	88°08′36″	29.2	6.71	3.90	7.66	5.6	0.178	6.64
HGH13/SGW-5	10.08.2013	Kakdwip (37 m)	21°51′11″	88°11′30″	30.2	7.31	2.24	4.39	−2.3	0.174	5.50
HGH13/SGW-6	11.08.2013	Kakdwip (15 m)	21°51′04″	88°19′25″	31.2	7.11	2.00	10.14	−10.6	0.191	2.39
HGH13/SGW-7	15.11.2013	Chemaguri (76 m)	21°40′05″	88°07′29″	30.0	8.12	0.72	8.79	−7.3	0.130	3.15
HGH13/SGW-8	16.11.2013	Light house (61 m)	21°39′23″	88°02′30″	28.1	8.14	0.52	7.94	−7.1	0.107	0.22
Effluent waters											
HGH13/P-1	05.05.2013	Garden reach	22°32′59″	88°17′38″	31.0	7.11	0.50	5.56	−3.6	NM	1.46
HGH13/P-2	05.05.2013	Majerhat	22°31′05″	88°19′29″	31.5	7.26	0.40	4.04	−9.7	0.089	1.47

(*continued on next page*)

Table 1 (*continued*)

Sample code	Date	Location	Latitude (N)	Longitude (E)	Temperature (°C)	pH	Salinity	DIC (mM)	$\delta^{13}C_{DIC}$ (‰ VPDB)	DO[#] (mM)	Ca (mM)
HGH13/P-3	05.05.2013	Babughat	22°34′00″	88°20′26″	31.0	8.10	0.17	2.14	−4.7	0.216	0.83
HGH13/P-4	31.05.2013	Durgachalk SBI	22°03′44″	88°08′28″	30.2	5.91	2.30	2.41	−5.3	0.191	2.13
HGH13/P-5	31.05.2013	IOCL effluent	22°03′14″	88°08′36″	30.2	6.19	2.47	2.84	−6.2	0.162	2.40
HGH13/P-6	31.05.2013	Durgachak jetty	22°03′25″	88°08′25″	30.0	5.63	2.66	2.27	−1.8	0.195	1.16

DIC – Dissolved inorganic carbon, DO – Dissolved oxygen, [L]Low tide, [M]Between low and high tide, [H]High tide, [DP]DO have been measured at different water depths for these samples, but only the surface water values presented here. NM – Not measured.
[#] DO has been measured in samples of only 2013 collection.

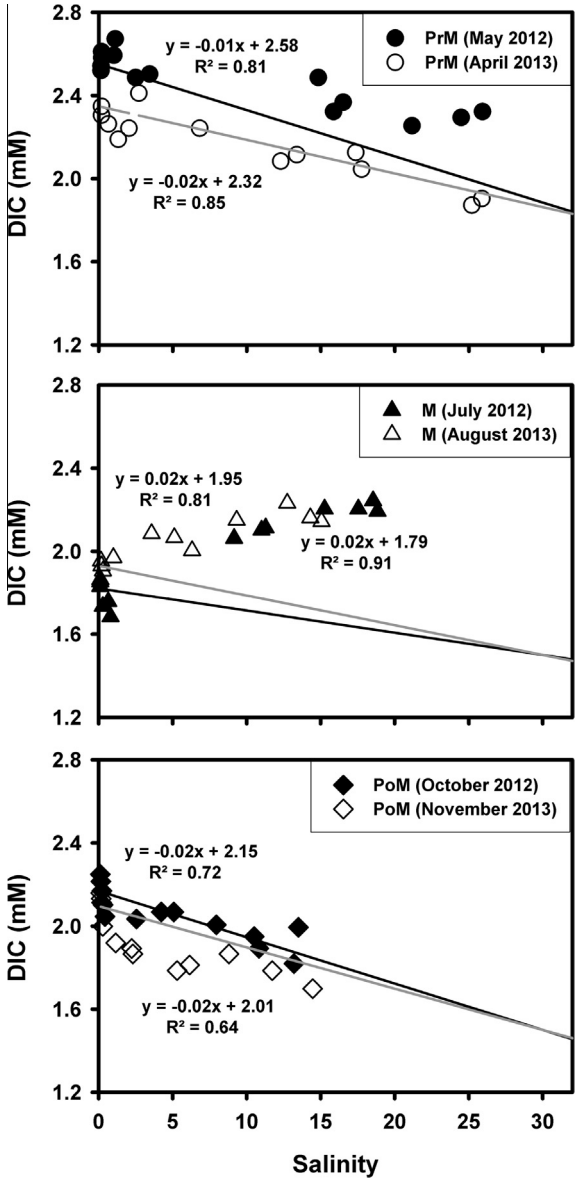

Fig. 3. Variation of concentrations of dissolved inorganic carbon (DIC) with salinity. The regression parameters are given, but regression lines are not shown. The plots show that at any given salinity, DIC concentrations are higher during the pre-monsoon (PrM) and post-monsoon (PoM) periods in the year 2012 than in the year 2013. The lines represent conservative mixing of freshwater and seawater using the end member composition given in Table 3. Note that in the monsoon period (M), all samples in the mixing zone plot far above the conservative mixing lines. The magnitudes of the errors are less than the symbol size.

(1.73–2.58 mM) compared to samples collected from its mouth at Gangasagar (1.79–2.32 mM; Table 1). The DIC concentrations of estuary water at Gangasagar are higher compared to the freshwaters only for samples collected during the monsoon period. For freshwaters ($S \leqslant 0.3$), pre-monsoon samples have the highest, and the monsoon samples have the lowest values of DIC concentrations, with post-monsoon samples having intermediate values. In general, during pre-monsoon and post-monsoon periods, the

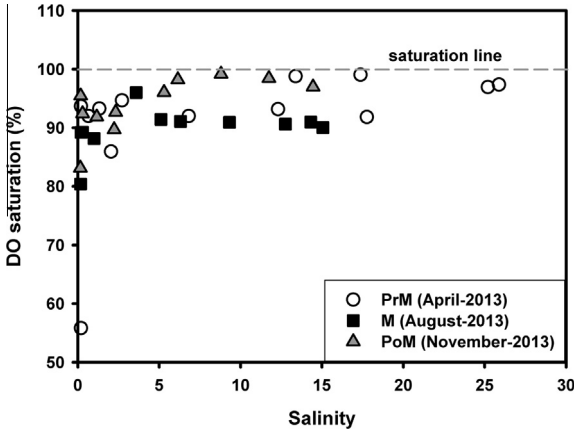

Fig. 4. Variation of oxygen saturation with salinity. The plot shows that all water samples are undersaturated with oxygen and that oxygen saturation increases with salinity.

DIC values at any given salinity were higher in the year 2012 than in the year 2013 (Table 1, Fig. 3). The observed DIC concentrations in the Hooghly River are higher than the DIC concentrations in other large rivers such as the Amazon (Quay et al., 1992), the Mississippi (Dubois et al., 2010), the Lena (Alling et al., 2012) and the Pearl (Guo et al., 2008). Dissolved O_2 concentrations in the Hooghly waters varied from 190 to 249 μM. One tributary, the Bethabati Khal (Table 1), draining primarily through industrialized areas, has the lowest dissolved O_2 concentration (131 μM). Calculations using the water temperature and data on oxygen solubility show that all samples have undersaturated O_2 concentrations (Fig. 4). For groundwater samples (Table 1), salinity ranged from 0.46 to 4.21 (mean = 1.82), dissolved Ca ranged from 0.22 to 6.64 mM (mean = 3.21 mM) and DIC varied from 4.39 to 11.21 mM (mean = 7.51 mM). In general, dissolved Ca and DIC concentrations are higher in groundwater than in the Hooghly waters. DO concentrations were lower in the groundwater.

The $\delta^{13}C_{DIC}$ values ranged from −11.4 to −1.6‰ for the Hooghly samples analyzed in this study (Table 1, Fig. 5). The fresh waters ($S \leqslant 0.3$) generally have lower $\delta^{13}C_{DIC}$ values (−11.4 to −4.0‰) than the waters collected at the mouth (−7.9 to −1.6‰). At any given location, the post-monsoon samples generally have the lowest $\delta^{13}C_{DIC}$ values, and the pre-monsoon samples have the highest $\delta^{13}C_{DIC}$ values (Fig. 6). $\delta^{13}C_{DIC}$ values of samples collected from the main channel of the Hooghly in this study are generally comparable with the time-series data of Ghosh et al. (2013) from one location in the Muriganga channel (Fig. 2). However, a few samples of Ghosh et al. (2013) showed very low $\delta^{13}C_{DIC}$ values (ca. −19‰). This issue is discussed later in greater detail in Section 5.5. Seasonal variations of $\delta^{13}C_{DIC}$ values in the fresh waters of the Hooghly River are comparable to those reported in the Scheldt estuary (−14.6 to −7.6‰; Hellings et al., 1999), and the St. Lawrence River system (2.2 to −13.7‰; Barth and Veizer, 1999).

The $\delta^{13}C_{POC}$ values in suspended sediments (Table 2) show less variation, from −24.9 to −22.4‰ (mean = −23.7 ± 0.8‰), which is similar to the mean $\delta^{13}C_{POC}$ of −22.5‰ (Aucour et al., 2006) reported for the Ganga and the Bramhaputra rivers in Bangladesh. In comparison, $\delta^{13}C_{POC}$ values of the Hooghly estuary are higher compared to those reported in other estuaries around the world, e.g., the Scheldt estuary (Hellings et al., 1999), the Lena River estuary (Alling et al., 2012) and Apalachicola Bay (Chanton and Lewis, 1999).The $\delta^{13}C_{POC}$ values in the Hooghly estuary are lower than the $\delta^{13}C$ values of marine phytoplankton (ca. −20‰) from the BoB (Fontugne and Duplessy, 1981; Rodelli et al., 1984).

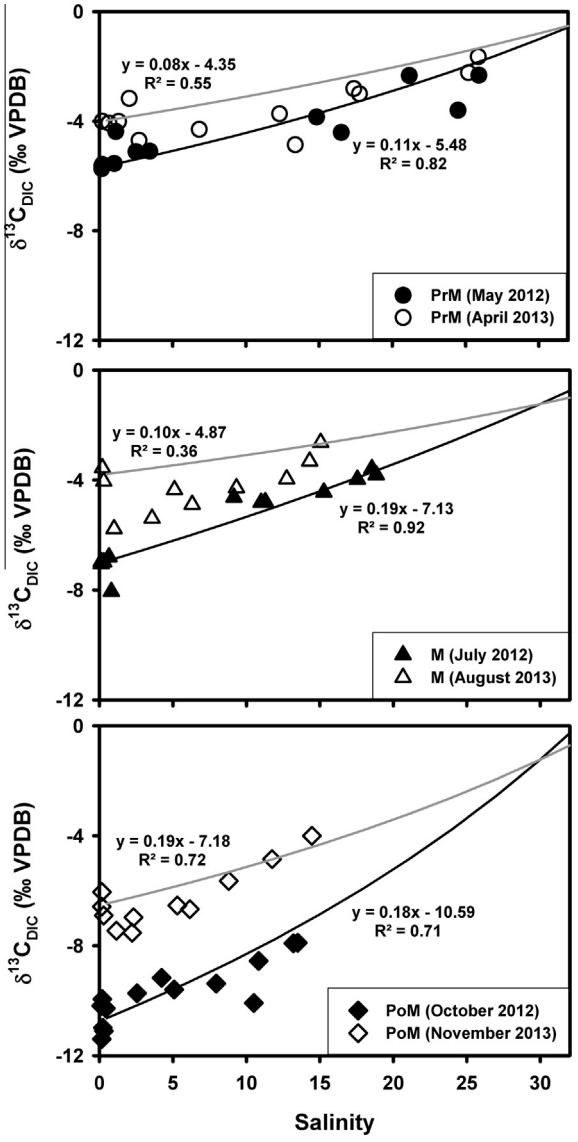

Fig. 5. Variation of $\delta^{13}C$ of dissolved inorganic carbon ($\delta^{13}C_{DIC}$) with salinity. The linear trends (regression lines not shown) suggest that mixing can account for most of the variability in the data. At any given salinity, the samples collected in the year 2012 have lower $\delta^{13}C_{DIC}$ compared to the samples collected in the year 2013. The lines represent conservative mixing of freshwater and seawater using the end member composition given in Table 3. The magnitudes of the errors are less than the symbol size.

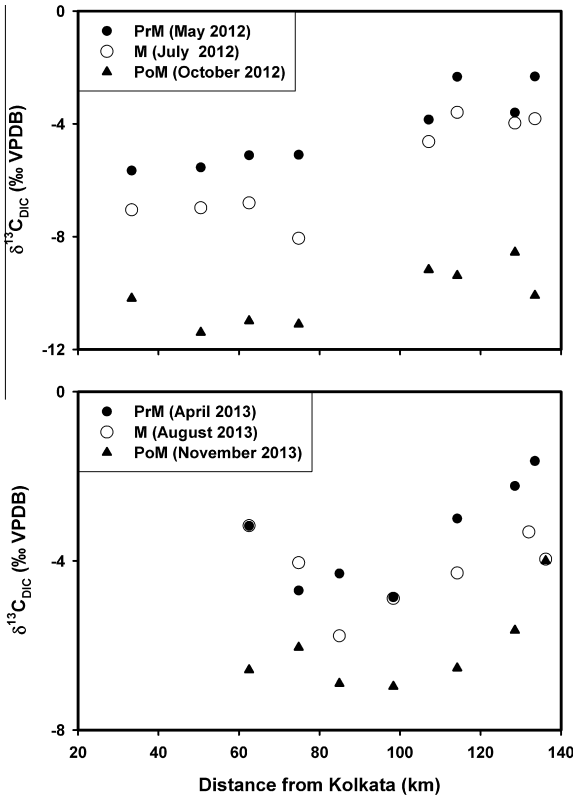

Fig. 6. Seasonal variation of $\delta^{13}C_{DIC}$ in the Hooghly estuary. The data show that, in general, pre-monsoon waters have the highest and post-monsoon waters have the lowest $\delta^{13}C_{DIC}$. However, $\delta^{13}C_{DIC}$ values also overlap between seasons for a few locations. Data for only those locations where sampling was performed for all three seasons are shown. The magnitudes of the errors are less than the symbol size.

5. DISCUSSION

DIC concentrations show significant negative correlation with salinity in the pre-monsoon and post-monsoon seasons, whereas a strong positive correlation is observed for the monsoon samples (Fig. 3). $\delta^{13}C_{DIC}$ values also show significant positive correlations with salinity in all seasons (Fig. 5). Note that in both of these plots, a significant number of data points lie off of the overall linear trends.

The measured DIC concentrations and $\delta^{13}C_{DIC}$ values in the estuary are a result of the combined influence of seawater-river water mixing, chemical weathering, supply of soil CO_2, CO_2 exchange with the atmosphere, biological production, precipitation or dissolution of minerals such as calcite, and respiration and degradation of organic matter, which may be supplied via both natural as well as anthropogenic processes. In the following, we use the data on DIC concentrations, $\delta^{13}C_{DIC}$ and $\delta^{13}C_{POC}$, dissolved Ca and O_2 concentrations, and estimates of river water pCO_2 and calcite saturation index obtained from thermodynamic calculations to delineate the processes responsible for the observed DIC and $\delta^{13}C_{DIC}$ variations in the estuary.

5.1. Mixing of river and seawater

Considering that mixing of river water and seawater occurs in the estuary, the abundance and distribution of nutrients, elements and isotopes are influenced by this process. The Hooghly estuary is reasonably well mixed, as evident from the observed strong linear covariation of salinity with the oxygen isotope composition ($\delta^{18}O$) of water (Somayajulu et al., 2002; Ghosh et al., 2013). The effect of mixing is readily apparent and is manifested in the gradual change of salinity along the mixing zone. DIC concentrations show significant to strong linear covariation with salinity (r^2: 0.64 to 0.91) (Fig. 3). The observed linear covariation suggests that mixing of seawater and river water accounts for most of the variability of DIC in the estuary in the non-monsoon periods. The linear trends defined by the data in the monsoon periods do not conform to the conservative mixing of the river and seawater.

As mentioned earlier, salinity and $\delta^{13}C_{DIC}$ also show significant linear covariation (r^2: 0.36 to 0.92), with the correlation being the strongest in the monsoon period of the year 2012 (Fig. 5). These covariation trends are mainly a result of mixing of river waters (lower $\delta^{13}C_{DIC}$) with seawater (higher $\delta^{13}C_{DIC}$), and support the contention that seawater-river water mixing accounts for most of the variability in the DIC and $\delta^{13}C_{DIC}$ values in the estuary. However, as observed in Fig. 3, there is significant scatter in these plots (Fig. 5).

Table 2
Carbon isotope composition of organic matter in the suspended sediment samples of the Hooghly estuary.

Sample No	Location	$\delta^{13}C_{org}$ (‰ VPDB)
HGH12–11	Burul	−24.6
HGH12–2	Kulpi	−23.3
HGH12–8	Sapkhali	−23.6
HGH12–9	Light House	−24.7
HGH12–10	Gangasagar	−24.5
HGH12–26	Achhipur	−24.6
HGH12–23	Raychalk	−23.8
HGH12–21	Kulpi‘	−23.4
HGH12–14	Kachuberia Ghat	−22.7
HGH12–15	Sapkhali	−22.6
HGH12–18	Mandirtala	−24.1
HGH12–39	Nurpur	−23.0
HGH12–37	Nischindipur	−23.5
HGH12–31	Kachuberia Ghat	−23.8
HGH12–30	Sapkhali	−24.3
HGH12–29	Mandirtala	−24.5
HGH12–27	Gangasagar	−24.6
HGH12–34	Bakkhali	−24.9
HGH13–4	Kakdwip Lot No. 8	−22.4
HGH13–6	Gangasagar	−23.6
HGH13–7	Light House	−22.6
HGH13–14	Falta	−22.9
HGH13–15	Diamond Harbour	−22.9
HGH13–16	Kulpi	−23.9
HGH13–18	Kakdwip Lot No. 8	−22.6
HGH13–20	Kakdwip Lot No. 8	−23.7

Table 3
End member values of DIC and $\delta^{13}C_{DIC}$ used in mixing model calculations.

Sampling period	River water			Seawater (Northern BoB)		
	DIC (mM)	$\delta^{13}C_{DIC}$ (‰ VPDB)	Salinity	DIC (mM)	$\delta^{13}C_{DIC}$ (‰ VPDB)	Salinity
Pre-monsoon-2012	2.55[a]	−5.7[b]	0.16[c]	1.83[d]	−0.43[f]	32.65[d]
Monsoon-2012	1.82[a]	−7.0[b]	0.12[c]	1.50[e]	−1.23[g]	30.00[h]
Post-monsoon-2012	2.17[a]	−10.7[b]	0.12[c]	1.50[e]	−1.23[g]	30.00[h]
Pre-monsoon-2013	2.35[a]	−4.0[b]	0.19[c]	1.83[d]	−0.43[f]	32.65[d]
Monsoon- 2013	1.93[a]	−3.8[b]	0.18[c]	1.50[e]	−1.23[g]	30.00[h]
Post-monsoon-2013	2.09[a]	−6.5[b]	0.16[c]	1.50[e]	−1.23[g]	30.00[h]

[a] Average DIC concentration of the samples collected at ⩽ 0.3 salinity (Table 1).
[b] Average $\delta^{13}C_{DIC}$ value of the samples collected at ⩽ 0.3 salinity (Table 1).
[c] Lowest salinity for a particular sampling period (Table 1).
[d] DIC concentration of the sample collected from northern BoB (13.01°N, 88.82°E) in the month of April–May during WOCE (1994–96) survey Sabine et al. (2002). This value is very similar to the DIC concentration of 1.88 mM reported for northern BoB (13.13°N, 88.74°E) in April 2007 (Ocean Carbon Dioxide Information analysis centre dataset, http://cdiac.ornl.gov/oceans/RepeatSections/clivar_i09n.html).
[e] Based on extrapolation of DIC at $S = 30$ using salinity and DIC data in the northern BoB in the month of December, 2010-January, 2011 Akhand et al. (2012). This DIC concentration is very similar to the data (1.59 ± 0.04 mM) reported for BoB (ca. 40 km east from the Mahanadi river mouth) during July–August, 2010. Sarma et al. (2012).
[f] δ^{13}CDIC at $S = 32.65$ for the month of November Dutta et al. (2010).
[g] δ^{13}CDIC at $S = 30.00$ for the month of November Dutta et al. (2010).
[h] Data based on Dutta et al. (2010) and Akhand et al. (2012).

To assess the deviation from conservative mixing, the DIC concentrations resulting from mixing of freshwater and seawater (DIC_{mix}) at various salinities were calculated using the following equation:

$$DIC_{mix} = DIC_f F_f + DIC_m(1 - F_f) \quad (1)$$

where subscripts m and f stand for seawater and freshwater, respectively. The fresh water fraction is designated as F_f and is calculated from salinity using the following equation:

$$F_f = 1 - \frac{[Sal]_s}{[Sal]_m} \quad (2)$$

where s and m refer to sample and seawater, respectively.

Similarly, considering both DIC and $\delta^{13}C$ values of river water and seawater end members, $\delta^{13}C_{DIC}$ resulting from conservative mixing ($\delta^{13}C_{DIC(mix)}$) were calculated using the equations of Mook and Tan (1991).

$$\delta^{13}C_{DIC(mix)} = \frac{Sal_s(DIC_f\delta^{13}C_f - DIC_m\delta^{13}C_m) + Sal_f DIC_m\delta^{13}C_m - Sal_m DIC_f\delta^{13}C_f}{Sal_s(DIC_f - DIC_m) + Sal_f DIC_m - Sal_m DIC_f} \quad (3)$$

where Sal stands for salinity; the subscripts s, m and f refer to sample, seawater and freshwater, respectively. F_f is the freshwater fraction as defined in Eq. (2). The end member compositions for various parameters (salinity, DIC and $\delta^{13}C_{DIC}$) used in Eqs. 1–3 are given in Table 3. The results of these calculations are plotted as mixing lines in Fig. 3 and Fig. 5. In Fig. 3, it can be seen that many of the measured DIC concentrations do not fall on the mixing lines. Most notable is the observation that in the monsoon periods of both years, the measured DIC concentrations are much higher than that predicted by the conservative mixing of freshwater and seawater. Similarly, in Fig. 5, it is observed that for a significant number of samples, measured values of $\delta^{13}C_{DIC}$ are lower than $\delta^{13}C_{DIC(mix)}$, although a few samples have $\delta^{13}C_{DIC} > \delta^{13}C_{DIC(mix)}$ (Fig. 5). Monsoon samples of the year 2012, however, generally show better agreement between $\delta^{13}C_{DIC}$ and $\delta^{13}C_{DIC(mix)}$ (Fig. 5).

It can be seen in Figs. 3 and 5 that the observed DIC and $\delta^{13}C_{DIC}$ values cannot be explained only by conservative mixing, indicating the importance of additional processes in the estuary. It is noteworthy that processes that bring about change in DIC and involve fractionation of carbon isotopes will also induce change in $\delta^{13}C_{DIC}$ values. It is thus required that these processes be looked into by considering both DIC and $\delta^{13}C_{DIC}$ together. Analogous to the approach of Alling et al. (2012), we calculated the deviations of measured DIC concentration (Δ[DIC]) and of $\delta^{13}C_{DIC}$ values ($\Delta[\delta^{13}C_{DIC}]$) from the values expected due to conservative mixing of seawater and river water.

$$\Delta[\delta^{13}C_{DIC}] = \delta^{13}C_{DIC(sample)} - \delta^{13}C_{DIC(mix)} \quad (4)$$

$$\Delta[DIC] = \frac{[DIC]_{sample} - [DIC]_{mix}}{[DIC]_{mix}} \quad (5)$$

where DIC_{mix} and $\delta^{13}C_{DIC(mix)}$ are estimated based on Eqs. (1) and (3), respectively. The estimated Δ[DIC] values are the highest for the monsoon samples, whereas lower and near zero values are observed for the post-monsoon samples (Fig. 7). It is noteworthy that Δ[DIC] values show a strong linear covariation with salinity for monsoon samples (r^2: 0.95–0.96 for both the years), suggesting that a higher amount of DIC is generated within the estuary in the high salinity region. This inference is not significantly changed even if a higher DIC value is used for the seawater end member than that used (Table 3) in the calculation of DIC_{mix}. In a plot of $\Delta[\delta^{13}C_{DIC}]$ vs. Δ[DIC] (Fig. 7), the origin represents the locus of samples whose DIC and $\delta^{13}C_{DIC}$ are influenced only by conservative mixing. Many of the samples analyzed in this study cluster around the origin, suggesting that for these samples conservative mixing accounts for nearly all of the variability in DIC and

$\delta^{13}C_{DIC}$. Samples that are influenced by additional biogeochemical and physical processes plot away from the origin in four different quadrants (see caption of Fig. 7 for details). In addition, several vectors were drawn that show the direction in which the data points would move if the samples were influenced by one or more processes. For example, if one sample was subject to outgassing of CO_2 subsequent to degradation of organic carbon, it will plot in the quadrant that is also indicative of calcite precipitation (see Fig. 7 and Appendix for details). In the following, we evaluate the importance of various processes (e.g., biological production, degradation of organic carbon, outgassing of CO_2, calcite precipitation and dissolution, groundwater contribution and anthropogenic activity) in influencing the DIC and $\delta^{13}C_{DIC}$ in the Hooghly estuary.

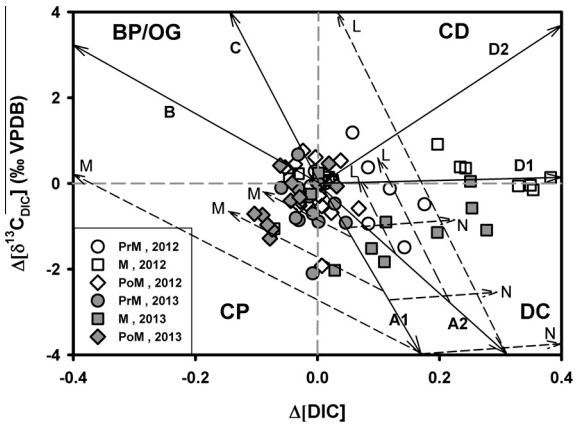

Fig. 7. Plot of $\Delta[\delta^{13}C_{DIC}]$ vs. Δ[DIC] in the Hooghly waters, where $\Delta[\delta^{13}C_{DIC}]$ and Δ[DIC] are deviations from the values expected from conservative mixing calculations based on Eq. (4) and (5) (see text). The origin is the locus of samples whose DIC and $\delta^{13}C_{DIC}$ are governed *only* by conservative mixing of seawater and river water. The figure is divided into four quadrants, each indicating the position of samples whose DIC and $\delta^{13}C_{DIC}$ have been influenced by additional processes. The quadrant DC represents degradation/oxidation of organic carbon, during which DIC concentrations increase and $\delta^{13}C_{DIC}$ values decrease. The quadrant BP/OG represents biological production/outgassing of CO_2, which causes DIC to decrease and $\delta^{13}C_{DIC}$ to increase. The quadrant CP represents calcite precipitation that results in a decrease of both DIC and $\delta^{13}C_{DIC}$. Calcite dissolution results in an increase of both DIC and $\delta^{13}C_{DIC}$, and causes the samples to plot in quadrant CD. The solid lines indicate the directions in which data points would move away from the origin if samples were subjected to *a specific* additional process. The dashed lines indicate the direction in which the samples would plot if they were subjected to *more than one* process. See Appendix for details on calculations and the drawing of these lines. Solid lines: Lines A1 and A2, drawn using the $\delta^{13}C_{DIC}$ of seawater and river water, respectively, indicate the effect of degradation of organic carbon. Line B indicates the effect of outgassing of CO_2. Line C indicates the effect biological production. Lines D1 and D2, drawn using the $\delta^{13}C_{DIC}$ of seawater and river water, respectively, indicate the effect of carbonate dissolution. Dashed lines: Lines marked L, which are drawn parallel to Line C, indicate the effect of degradation of organic carbon followed by biological production, Lines marked M, which are drawn parallel to Line B, indicate the effect of organic degradation of carbon followed by outgassing of CO_2. Lines marked N, which are drawn parallel to Line D1, indicate the effect of degradation of organic carbon followed by carbonate dissolution. Most of the samples in the low salinity zone cluster around the origin, whereas samples from the high salinity zone ($S \geqslant 10$), particularly for the monsoon period, plot far away from the origin and show signatures of organic carbon degradation and carbonate dissolution (see text). A few samples of the post-monsoon period of the year 2013 plotted in quadrant CP have been influenced by outgassing of CO_2 followed by degradation of organic carbon. The magnitudes of the errors are less than the symbol size.

5.2. Biological productivity

Previous studies have reported data on biological productivity in the Hooghly estuary (De et al., 1991; Mukhopadhyay et al., 2002; Choudhury and Pal, 2012). Considering that nutrient supply is not limited in the estuary, variation in plankton productivity primarily results from changes in the depth of the photic layer, which is influenced by the magnitude of sediment suspension. Intense sediment suspension during the pre-monsoon and monsoon periods leads to a decrease in the depth of the photic layer and is responsible for decreased plankton productivity compared with the post-monsoon period (De et al., 1991; Mukhopadhyay et al., 2002; Choudhury and Pal, 2012). The depth of light penetration expressed as the Secchi disc depth was reported to be the highest during the post-monsoon period in mangrove-dominated estuaries in close proximity to the Hooghly estuary (Biswas et al., 2007; Dutta et al., 2015). Most of the studies report that productivity is the highest during the post-monsoon period, not only in the Hooghly estuary (Mukhopadhyay et al., 2002; Choudhury and Pal, 2012; Mandal et al., 2012; Banerjee, 2012) but also in the nearby mangrove-dominated estuaries draining through the Sunderbans (Biswas et al., 2007; Dutta et al., 2015). In Fig. 7, a few samples plot in quadrant (BP/OG) that is indicative of both biological production and outgassing of CO_2. As both of these processes lead to the loss of DIC

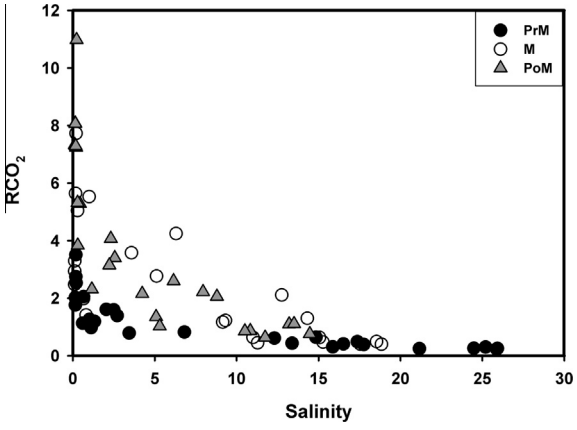

Fig. 8. Variation of RCO_2 (=calculated pCO_2 in waters/pCO_2 of the atmosphere) with salinity. The details on the calculation of pCO_2 are given in the text. The data show that many of the waters, particularly in the low salinity zone, are characterized by high pCO_2, whereas pCO_2 values drop to near atmospheric levels or lower in the high salinity zone ($S \geqslant 10$).

and preferential removal of ^{12}C from the DIC pool, the result of these processes is an increase in $\delta^{13}C_{DIC}$ and decrease in DIC. Thus, samples subject to one or both of the processes plot in the same quadrant (BP/OG). Although it is difficult to separate the effect of biological productivity and outgassing of CO_2 in samples plotting in quadrant BP/OG, results of this investigation and from reported studies indicate that primary production is less important in regulating the DIC and $\delta^{13}C_{DIC}$ values in the Hooghly estuary. First, during the post-monsoon period, a time of maximum biological productivity, measured $\delta^{13}C_{DIC}$ values in the estuary are the lowest among all of the seasons (Figs. 5, 6) and are generally lower than the calculated values for $\delta^{13}C_{DIC(mix)}$ (Fig. 7).This is in contrast to what would be expected from the response of DIC and $\delta^{13}C_{DIC}$ to biological production. Second, it has been reported that because of the high turbidity and rather shallow depth of the euphotic layer (<1 m), the Hooghly estuary remains heterotrophic throughout the year (Mukhopadhyay et al., 2002). This is also evident from the dissolved O_2 concentrations that are mostly at undersaturated levels during all of the sampling periods (Fig. 4). Undersaturated DO levels support inferences drawn from earlier studies that respiration and degradation of organic carbon dominate over primary production in the estuary. It is likely that the overall effect of biological productivity on DIC and $\delta^{13}C_{DIC}$ was offset by respiration and degradation of organic carbon, the latter exerting the opposite effect. The observation that a large number of samples plot in quadrant DC, which is suggestive of organic carbon degradation, and that only a few samples plot in quadrant BP/OG (Fig. 7), which is indicative of biological productivity, reinforces the inference that the role of biological production is less significant than degradation of organic carbon in influencing the DIC and $\delta^{13}C_{DIC}$ of the Hooghly estuary.

5.3. Precipitation of carbonate minerals

Precipitation of carbonate minerals such as calcite can influence the DIC concentrations and $\delta^{13}C_{DIC}$ values because ^{13}C is preferred over ^{12}C as DIC is incorporated into the mineral (Romanek et al., 1992). A few samples indeed plot in the quadrant CP, suggestive of calcite precipitation (Fig. 7). However, it is noteworthy that samples that were subjected to degradation of organic carbon followed by outgassing of CO_2 would also occupy the same area in this plot. To assess whether calcite precipitation is an ongoing process in the Hooghly estuary waters, we estimated the saturation index of calcite (SI_{cal}) using the measured temperature and calculated ionic strength by the following formula:

$$SI_{cal} = \log\left(\frac{IAP}{K_{sp}}\right) \quad (6)$$

Ion activity product (IAP) was calculated using the activity of Ca^{2+} and CO_3^{2-} in the waters. The Extended Debye–Huckel and Davies equations were used to calculate the activity coefficient of dissolved species at low (<0.1 M) and high (>0.1 M) ionic strengths, respectively. The solubility product of calcite (K_{sp}) across the range of salinities measured in the estuary was calculated using the equations of Mucci (1983). The calculations show that only 14 out of 77 samples have $SI_{cal} > 0$. Considering the errors in the measurements and calculations, if a value of $SI_{cal} > 0.2$ is taken as the measure of supersaturation, only seven samples qualify for this criterion of supersaturation. The pre-monsoon water samples, particularly for the year 2012, are characterized by higher DIC concentrations, higher temperatures and mostly positive values of SI_{cal}, and thus have the greatest potential for calcite precipitation. However, these waters are characterized by higher $\delta^{13}C_{DIC}$ values (Fig. 6). In addition, it is observed that a few samples of the post-monsoon period of the year 2013 plot significantly away from the origin in quadrant CP (Fig. 7), which is indicative of both calcite precipitation as well as CO_2 outgassing followed by degradation of organic carbon. However, these samples have $SI_{cal} < 0$, suggesting that CO_2 outgassing rather than calcite precipitation is responsible for their observed values of DIC and $\delta^{13}C_{DIC}$. These observations, together with the estimated values of SI_{cal}, suggest that calcite precipitation was not an important ongoing process in the Hooghly estuary during the periods of sampling.

5.4. Outgassing of CO_2 from the estuary

Levels of pCO_2 in river and estuary waters that are higher than atmospheric value can cause escape of CO_2 to the atmosphere. The outgassing of CO_2 from the estuary waters can bring about change in $\delta^{13}C_{DIC}$ values, as ^{12}C is preferentially lost during outgassing (Doctor et al., 2008; van Geldern et al., 2015). Estimates of pCO_2 in the Hooghly waters were made using the following equations.

$$[H_2CO_3] = K_{CO_2} \times pCO_2 \quad (7)$$

$$[H_2CO_3] \times K_1 = [H^+] \times [HCO_3^-] \quad (8)$$

$$[HCO_3^-] \times K_2 = [H^+] \times [CO_3^{2-}] \quad (9)$$

where [] represents the activity of individual species. Measured salinity and temperature were used to calculate the dissociation constants of the dissolved species. K_{CO_2} was calculated based on the approach of Weiss (1974). K_1 and K_2 were calculated using the equations developed by Mook and Koene (1975) and further modified by Cai and Wang (1998). These equations hold for the salinity range from 0 to 40. The calculations show that waters are characterized by pCO_2 in the range of ~100 to ~4400 μatm, with an average pCO_2 of ~950 μatm. For many of the samples (51 out of 77), estimated pCO_2 is higher than atmospheric pCO_2. For freshwater samples, the pCO_2 values are generally much higher than the atmospheric pCO_2, whereas the pCO_2 values drop to near atmospheric levels or lower for samples collected from the high salinity zone in the estuary (Fig. 8). All samples of the post-monsoon season (except four) have pCO_2 higher than the atmospheric value, whereas several samples collected during the pre-monsoon and monsoon periods have pCO_2 values that are lower than atmospheric pCO_2. If outgassing of CO_2 is indeed an important process in the Hooghly estuary, associated

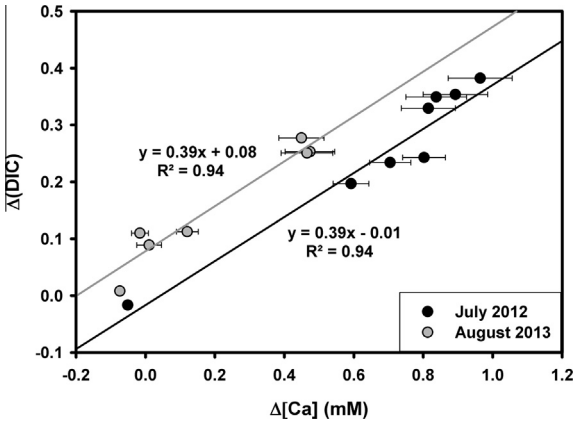

Fig. 9. Plot of Δ[DIC] vs. Δ[Ca] for monsoon samples. A strong positive correlation between these two parameters suggests that DIC is generated in the estuary via carbonate mineral dissolution. The composition of freshwater is based on the average of the data at $S \leqslant 0.3$. The regression of the data does not take into account the error of the estimates. See Section 5.6 for calculation and detailed discussion.

changes in DIC and $\delta^{13}C_{DIC}$ would be reflected in the $\Delta[\delta^{13}C_{DIC}]$ vs. Δ[DIC] plot (Fig. 7). It is, however, observed that only a few samples plot in quadrant BP/OG, which is characteristic of outgassing. The plot also shows that a few samples of the post-monsoon period of the year 2013 that plotted in quadrant CP may have lost CO_2 subsequent to being subjected to degradation of organic carbon. Mukhopadhyay et al. (2002), however, suggested that CO_2 outgassing from the estuary was important only during the pre-monsoon period. This is not supported by the data and calculations of this study. The results of this study suggest that overall outgassing of CO_2 is an ongoing but not an important process in regulating the DIC and $\delta^{13}C_{DIC}$ of the Hooghly estuary, although it seems to be operating in tandem with other processes such as degradation of organic carbon, particularly in the post-monsoon period (see the Section 5.5). A large majority of samples of this study have near atmospheric or lower pCO_2 values in the high salinity ($S \geqslant 10$) waters (Fig. 8). It is tempting to suggest outgassing of CO_2 as the cause of low pCO_2 in these samples. However, observation of considerable DIC excess (Δ [DIC]) in these samples is in contrast with what would be expected from outgassing of CO_2. In Section 5.6, we explain that carbonate dissolution followed by degradation of organic carbon is responsible for low pCO_2 in high salinity waters.

5.5. Degradation of organic carbon and biological respiration

It is striking that in a plot of $\Delta[\delta^{13}C_{DIC}]$ vs. Δ[DIC], a large majority of the samples plot in the field DC, which is suggestive of degradation of organic carbon (Fig. 7). The observation that most of the samples analyzed exhibit undersaturated values for dissolved O_2 concentrations (Fig. 4) suggests that organic carbon degradation and respiration exceed biological production in the estuary. This inference is supported by reported values of productivity and respiration in the Hooghly estuary (De et al., 1991; Mukhopadhyay et al., 2006; Choudhury and Pal, 2012) with an average productivity-respiration (P/R) ratio of 0.49 (Mukhopadhyay et al., 2006). These results, together with the observation that for a large number of samples, particularly for the monsoon collection of the year 2013, measured $\delta^{13}C_{DIC}$ values are lower than the values expected from conservative mixing (Figs. 5 and 7), suggest that respiration and degradation of organic carbon is one of the dominant processes contributing to the variability in DIC and $\delta^{13}C_{DIC}$ values in the Hooghly estuary. This inference is consistent with the lowest values of (P/R) ratio during the monsoon period reported in the Hooghly (Mukhopadhyay et al., 2006) and in the nearby estuaries (Biswas et al., 2007). However, the effect of seasonal variation in biological respiration on $\delta^{13}C_{DIC}$ may have been further modified if the water samples were subsequently subjected to processes such as carbonate dissolution and CO_2 outgassing. It is noteworthy that dissolved O_2 concentrations do not show any significant covariation with $\delta^{13}C_{DIC}$ values. This is not unexpected, considering that DIC and dissolved O_2 in the waters are a result of combined effects of several processes including exchange with the atmosphere, biological production and respiration, and degradation of organic carbon.

As mentioned earlier, the $\delta^{13}C_{DIC}$ values for freshwaters ($S \leqslant 0.3$) decreased from −5.7‰ in the pre-monsoon period to −11.4‰ in the post-monsoon period. It is observed that calculated values of RCO_2, defined as the ratio between aqueous pCO_2 and atmospheric pCO_2, are lower in the pre-monsoon samples, particularly for fresh and low salinity waters (Fig. 8). In addition, $\delta^{13}C_{DIC}$ values show significant negative covariation with RCO_2 in the mixing zone ($S > 0.3$) during all three sampling periods. All this, together with the observation of high values of DIC in fresh waters, suggests that in the monsoon and post-monsoon period, higher supply of soil CO_2, which is characterized by lower $\delta^{13}C$, is contributing to the lower and variable $\delta^{13}C_{DIC}$ values in the freshwaters. Flushing of soil CO_2 is likely more efficient during monsoon and post-monsoon periods, when there is higher rainfall and discharge. Smaller deviations from the conservative mixing values of DIC and $\delta^{13}C_{DIC}$ in the low salinity region ($S \leqslant 0.5$), as evident from near zero values of Δ[DIC] and $\Delta[\delta^{13}C_{DIC}]$ (Fig. 7), suggest that biological degradation is less significant in the freshwaters, and reinforce the idea that low $\delta^{13}C_{DIC}$ values of freshwater samples are primarily inherited from the supply of soil CO_2. It is interesting to note that fractions of labile organic matter in particulate and dissolved organic carbon are the lowest in the post-monsoon periods (September to October) in the Ganga River waters in Bangladesh (Ittekkot et al., 1985). These observations, in conjunction with the finding that post-monsoon samples have the lowest $\delta^{13}C_{DIC}$ values (Table 1, Fig. 5), indicate that a significant fraction of the organic matter in this period has contributed to the DIC pool via biodegradation. Some of the post-monsoon samples of the year 2013 plotted in quadrant CP are inferred to have been subjected to outgassing of CO_2 subsequent to degradation of organic carbon (Fig. 7), given that carbonate precipitation is unlikely

(as evident from calcite undersaturation in these samples). High values of Δ[DIC], particularly for monsoon samples in the high salinity waters ($S \geqslant 10$), can be generated by biological respiration and degradation of organic carbon. However, lower values of RCO_2 in these waters indicate that additional process(es) are required to explain high values of Δ[DIC]. The most likely process that can bring about the observed changes in RCO_2, DIC and $\delta^{13}C_{DIC}$ is carbonate dissolution, as discussed in Section 5.6.

Ghosh et al. (2013) suggested that anaerobic oxidation of organic matter could also be influencing the $\delta^{13}C_{DIC}$ values in the Hooghly estuary. They cited evidence of anoxic conditions in the estuary based on the presence of H_2S in pore water. It is noteworthy that the presence of H_2S is very common in pore water, considering that oxygen is rapidly consumed via oxidation of organic matter in the sediment column. Thus, the presence of H_2S in the pore water is not necessarily an indication of the prevalence of anoxic condition in the overlying water column. The observation that dissolved O_2 concentrations in the surface water of the estuary are not very different than those in the bottom water (Sadhuram et al., 2005) provides support to the contention that anoxic conditions do not prevail in the water column of the estuary. Ghosh et al. (2013) also cite the occurrence of CH_4 reported by Biswas et al. (2007), and contend that oxidation of this methane could be a source of the lower $\delta^{13}C_{DIC}$ values observed in their study. Using the DIC concentrations in the Hooghly estuary (1.79–2.59 mM, Table 1) and the maximum reported methane concentrations in the nearby estuaries (60–70 nM; Biswas et al., 2007; Dutta et al., 2015), the effect of methane oxidation on $\delta^{13}C_{DIC}$ values in the estuary can be evaluated. Assuming that *all* methane is oxidized to produce DIC, it is estimated that methane oxidation can contribute a maximum of 0.003–0.004% of the total DIC pool. Using a value of −50‰ for the $\delta^{13}C$ of methane, it is estimated that methane oxidation could lower the measured $\delta^{13}C_{DIC}$ value by ca. 0.002‰, which cannot be distinguished within the analytical uncertainty. Although non-quantitative oxidation of methane may produce CO_2 with lower values of $\delta^{13}C$ due to isotopic fractionation, it has been observed that isotopic fractionation becomes significant in causing enrichment of ^{13}C in the residual methane only when the fraction of oxidized methane is more than 90% (Whiticar and Faber, 1986). This, together with the observation that methane concentrations in the nearby estuaries are very low, suggests that the overall effect of methane oxidation cannot be considered significant in influencing the $\delta^{13}C_{DIC}$ values in the estuary.

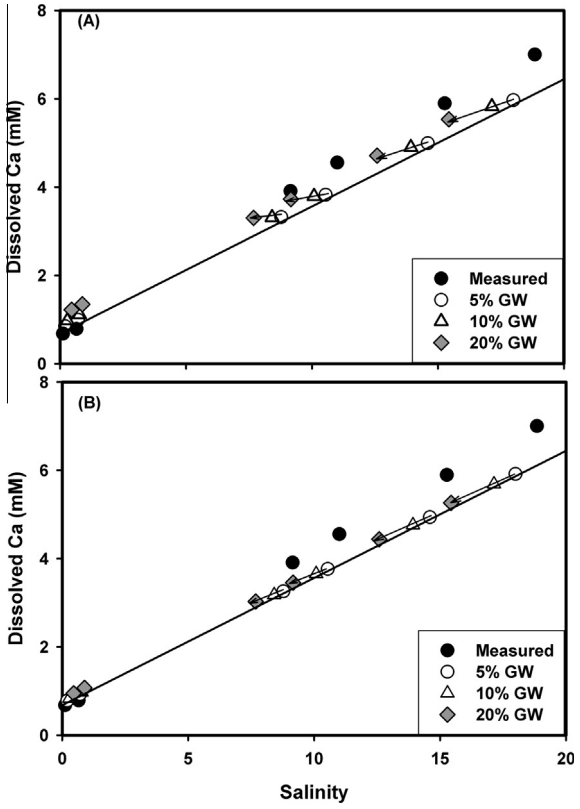

Fig. 10. Plot of dissolved Ca vs. salinity in the Hooghly waters for the monsoon period of the year 2012. The freshwater compositions are based on the average of data of samples with $S \leqslant 0.3$. The conservative mixing is represented by the lines shown. Also shown are the calculated compositions of freshwater-seawater-groundwater mixtures with different proportions of groundwater. (A) Calculations based on salinity and the average dissolved Ca of groundwater (3.21 mM) measured in this study (Table 1). (B) Calculations based on the average dissolved Ca concentrations of the groundwater from the GB plains (1.85 mM), estimated from the data of groundwater flux and associated Ca flux reported by Dowling et al. (2003). It is seen that with increasing proportions of groundwater, the salinity and Ca of the mixture decrease as indicated by arrows. Thus, the observed salinity and Ca distribution cannot be accounted for by groundwater contribution, particularly at high salinity. The magnitudes of the errors for measured Ca concentrations are less than the symbol size.

5.6. Carbonate dissolution

Considering that many of the waters are at or below calcite saturation ($SI_{cal} \leqslant 0$), dissolution of calcite from the suspended particles is not unlikely. As calcite dissolution would add DIC and increase $\delta^{13}C_{DIC}$ in water, samples subjected to this process will plot in quadrant CD in Fig. 7 if they were not influenced by additional processes. Processes such as respiration and biological degradation, however, would result in contrasting changes in DIC and $\delta^{13}C_{DIC}$, and thus make it difficult to assess the effect of carbonate dissolution. It is interesting to see that a few samples from the monsoon collection indeed plot in quadrant CD, which is indicative of carbonate dissolution (Fig. 7). All samples from the monsoon collection in the high salinity region ($S \geqslant 10$) have $SI_{cal} < 0$ and are most likely to experience the effect of calcite dissolution. Dissolution of calcite would supply additional Ca, and thus would result in non-conservative behavior of Ca in the estuary. A value of 10.12 mM for Ca concentration in the northern Bay of Bengal (BoB) was estimated based on the average Ca/Cl ratio (Sen Gupta et al., 1978). Mixing calculations using this value and measured Ca in the freshwater of the Hooghly River (Table 1) show that excess Ca (in excess of what can be sustained by conservative mixing) is

Table 4
Water budget of the Hooghly estuary and flux to the Bay of Bengal (BoB).

Season	V_q (10^8 m^3/day)[I]	V_p (10^7 m^3/day)[II]	V_e (10^6 m^3/day)[III]	V_w (10^5 m^3/day)[IV]	V_r (10^8 m^3/day)	V_x (10^8 m^3/day)[V]	Residence time (day)
Pre-monsoon, 2012	1.15	1.07	4.16	11.5	1.29	1.42	30.2
Monsoon, 2012	3.58	6.33	1.70	11.5	4.22	3.57	10.5
Post-monsoon, 2012	1.28	0.91	4.16	11.5	1.40	0.59	41.2
Pre-monsoon, 2013	1.15	1.07	4.16	11.5	1.29	1.42	30.2
Monsoon, 2013	3.58	6.33	1.70	11.5	4.22	2.58	12.1
Post-monsoon, 2013	1.28	0.91	4.16	11.5	1.40	0.66	39.9

[I] Calculated using the Hooghly water flow at Nabadwip (Fig. 2) reported by Rudra (2014). These values are 1336 m^3/s, 4141 m^3/s and 1483 m^3/s during pre-monsoon, monsoon and post-monsoon, respectively.
[II] Calculated using the average daily rainfall in the last 5 years (2009–2013) IMD (2013). These values are 1.78 mm, 10.55 mm and 1.51 mm during the pre-monsoon, monsoon and post-monsoon season, respectively.
[III] Based on the evaporation data Banerjee (2012).
[IV] Based on the waste water discharge of 1154 million liters/day Sadhuram et al. (2005).
[V] Calculated based on Eq. (12) using S_r = salinity at Gangasagar and Freserganj Mohana (Table 1), S_{ocean} = salinity of BoB (Table 3) and $S_{estuary}$ = mean salinity of the samples collected from the estuary in a particular season (Table 1).

observed for all seasons. Additional evidence of carbonate dissolution, particularly in the monsoon period, comes from the plot of Δ[DIC] vs. Δ[Ca], which shows a strong positive correlation ($r^2 = 0.94$, Fig. 9). Together, these observations lend support to the inference that carbonate dissolution is prevalent in the estuary and is responsible for generation of DIC. Using a representative average suspended particle concentration of 1 g/L, it is calculated that up to ca. 9 wt% calcium carbonate in the suspended particles is required to account for the maximum observed excess Ca (0.94 mM) in the monsoon period. However, the calcium carbonate concentrations in the suspended particles required to account for excess Ca would be lower if (i) the suspended particle concentrations are higher than the value used in the above calculation. Sinha et al. (2004), based on results of numerical modelling, reported higher values of suspended particle concentrations (e.g., 2.2–3.8 g/ℓ). (ii) A part of the excess Ca is supplied by other processes/sources such as desorption via cation exchange between the dissolved and the particulate phases, and groundwater contributions. Leaching experiments using dilute acid (1.5 M HCl), which provide estimates of maximum carbonate content, were carried out on several bottom sediments from the Hooghly estuary. This yielded carbonate contents in the range of ca. 10–20 wt%, consistent with the data (ca. 6–18 wt%) of Banerjee (2012). Thus, data on the carbonate content of sediments and the calculations made above together suggest that the carbonate present in the suspended particulate matter can indeed supply excess Ca. The excess Ca concentrations in the non-monsoon periods do not show any significant covariation with Δ[DIC]. Thus, the observations of this study suggest that carbonate dissolution is important in generating DIC in the estuary, particularly during the monsoon period. In the non-monsoon periods, the sources of excess Ca and DIC could be variable and decoupled. We speculate that cation exchange between the dissolved phase and the suspended particulate matter in the estuary may be another process that could release Ca from the latter via desorption, and thus can account for a part of the observed excess Ca.

Dissolution of carbonate minerals was also reported in other estuaries, e.g., the Gautami-Godavari estuary (Bouillon et al., 2003), the Loire (Abril et al., 2003) and the Ems estuary (de Jonge and Viilerius, 1989). However, Abril et al. (2003) observed carbonate dissolution in the low salinity region, whereas Bouillon et al. (2003) and de Jonge and Viilerius (1989) observed this effect in the low to middle salinity zone. In the present study, very high values of excess Ca were observed in the monsoon period at salinity $\geqslant 10$. This requires one or a combination of factors that cause re-suspension of estuary and/or marine sediments in the estuary at higher salinity. It has been reported that the depth of the estuary varies among the seasons and is shallower near the mouth than in the upper estuary (CIFRI, 2012). For example, the estuary is 14 m (45 ft) shallower near the mouth than at Diamond Harbour. This could result in higher turbulence and sediment re-suspension in the high salinity region, which may become amplified in the monsoon season due to higher water discharge. In addition, wind stress vectors and surface currents during the monsoon period are directed into the estuary, whereas in the post-monsoon period they are directed away from the estuary (Unger et al., 2003; Achyuthan et al., 2013). Thus, a combination of factors and processes—shallow depth near the mouth, higher water discharge in the monsoon, wind and surface current being directed into the estuary—all result in higher turbulence, re-suspension of estuary sediments and likely transport of marine sediments into the estuary and their re-suspension during the monsoon period. All this, together with the observation of calcite undersaturation in the monsoon period, would support higher carbonate dissolution in the high salinity

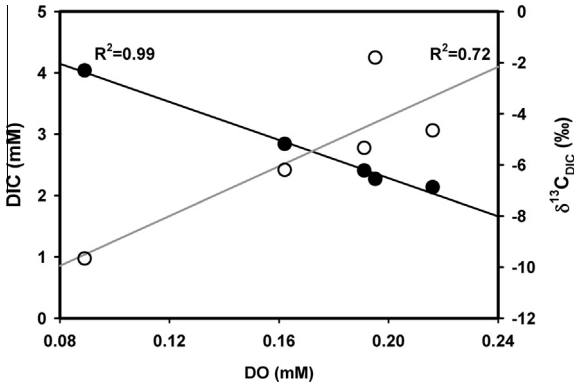

Fig. 11. Plot of DIC concentrations (filled circles) and $\delta^{13}C_{DIC}$ (open circles) vs. dissolved oxygen (DO) concentrations in industrial effluent and urban wastewaters that drain into the Hooghly estuary. An increase in DIC with decreasing DO is suggestive of generation of DIC via degradation of organic carbon sourced from industry and pollution. This is supported by a negative correlation observed between $\delta^{13}C_{DIC}$ and DO in these waters. The magnitudes of the errors are less than the symbol size.

region as inferred earlier based on calculated excess Ca concentrations. It is observed that very high values of Δ[DIC] for monsoon samples at $S \geqslant 10$ are not accompanied by higher $\Delta[\delta^{13}C_{DIC}]$ values (Fig. 7). It is noteworthy that carbonate dissolution followed by degradation of organic carbon can result in negative values of $\Delta[\delta^{13}C_{DIC}]$ as indicated by the vector N (Fig. 7). Based on the observation that many of the monsoon samples with high values of Δ[DIC] exhibit lower values of $\Delta[\delta^{13}C_{DIC}]$, we contend that both of these processes are operating together in the Hooghly estuary waters. The cause of significant excess Ca in non-monsoon periods remains uncertain. Although some of this excess Ca could be supplied by carbonate dissolution, a lack of significant covariation between excess Ca and Δ[DIC] does not allow us to interpret that carbonate dissolution is the only causative mechanism for the estimated excess Ca. As mentioned earlier, desorption may be a significant process in supplying a part of the excess Ca during the non-monsoon periods.

5.7. Groundwater contributions

Groundwater can contribute to the elemental and isotope budget of the Hooghly estuary if it is fed by aquifers. Submarine groundwater discharge (SGD) has been shown to be important in contributing to the abundance and distribution of selected elements (e.g., Ba) and isotopes (e.g., ^{226}Ra) at the mouth of the Ganga–Brahmaputra system in Bangladesh (Moore, 1997). In the Hooghly estuary, the observed non-conservative behavior of Ra isotopes has been explained by desorption from the estuary sediments (Somayajulu et al., 2002). In this study, we have sampled and analyzed shallow groundwater collected in areas adjacent to the estuary (Fig. 2; Table 1). It is observed that DIC and Ca concentrations in the groundwater samples are significantly higher than those in the estuary. Basu et al. (2001) suggested a groundwater contribution of 19% to the surface water flux from the Ganges–Brahmaputra floodplain. Using the measured salinity and Ca concentrations in this study, calculations were made for mixing of different proportions of groundwater (5–20%) with the river water-seawater mixture. These calculations (Fig. 10) indicate that groundwater contributions cannot account for the measured dissolved Ca at higher salinity ($S > 10$), although at lower salinity groundwater contributions may be sufficient to account for the measured Ca. Note that adding higher proportions of groundwater results in lower Ca and salinity in the mixture. Thus, groundwater contributions cannot account for the measured Ca in the high salinity waters where excess Ca is higher. Using Ca concentrations estimated from data of groundwater flux from the Ganges–Brahmaputra delta, and the associated Ca flux (Dowling et al., 2003), it is seen that groundwater contributions cannot account for measured Ca even in the low salinity region (Fig. 10).

Although the results of mixing calculations suggest that groundwater can be a potential source of Ca and DIC in the low salinity water of the Hooghly estuary, available data on Ra isotopes (Somayajulu et al., 2002) do not provide evidence of groundwater contributions to the estuary. Additional work employing tracers such as $^{87}Sr/^{86}Sr$ needs to be carried out for quantification of groundwater contributions to the Hooghly waters. The data on groundwater contributions can be used to determine if it can be a significant source of excess Ca observed in the non-monsoon periods.

5.8. Anthropogenic processes

Occurrence of anthropogenic carbon, such as charcoal, naphtha, petroleum and persistent organic pollutants (POP), has been reported in the Hooghly estuary sediment (Guzzella et al., 2005). Thus, the dissolved inorganic carbon in the Hooghly estuary may contain contributions from anthropogenic sources. We assess the role of pollution in the DIC budget of the Hooghly River based on analysis of a few samples of industrial effluent and wastewater collected from the vicinity of Haldia and Kolkata that drain into the Hooghly estuary (Table 1, Fig. 2). Using the wastewater and effluent discharge of 13.4 m^3/s (Sadhuram et al., 2005), the annual average water discharge from the Hooghly River (Table 6), and the maximum effluent DIC concentration of 5.56 mM (Table 1), it is estimated that the average contribution of anthropogenic activity to the measured DIC concentration could be 0.03 mM. This estimate becomes ca. 0.06 mM during non-monsoon periods when the river water discharge (Table 4) is smaller. The estimated DIC contributions from anthropogenic activity constitute ca. 2–3% of the river water DIC concentrations (Table 3). Concentrations of dissolved oxygen in the polluted effluents show strong negative correlation with DIC ($r^2 = 0.99$) and significant positive correlation with $\delta^{13}C_{DIC}$ ($r^2 = 0.72$, Fig. 11). A first order interpretation of this observation would be oxidative degradation of organic carbon that contributes to the DIC pool with a lower $\delta^{13}C$. Although these observations cannot be directly linked to the supply of organic carbon via pollution, they provide circumstantial evidence for contributions to DIC via

Table 5
DIC budget of the Hooghly estuary and DIC flux to the Bay of Bengal (BoB).

Season	V_q DIC_q (10^{10} mol)[I]	V_r DIC_r (10^{10} mol)[II]	V_x DIC_x (10^{10} mol)[III]	DIC Addition/ Removal (10^{10} mol)	Annual DIC Discharge (10^{10} mol)	% annual DIC addition	% annual DIC discharge
Pre-monsoon, 2012	3.53	3.60	4.36	4.43	7.96	27.40	25.81
Monsoon, 2012	7.81	11.1	7.95	11.2	19.02	69.46	61.73
Post-monsoon, 2012	3.34	3.27	0.57	0.51	3.84	3.14	12.46
Total (2012)				16.14	30.8		
Pre-monsoon, 2013	3.26	2.95	3.58	3.27	6.53	29.91	25.40
Monsoon, 2013	8.29	1.13	4.22	7.23	15.50	66.08	60.38
Post-monsoon, 2013	3.21	3.00	0.65	0.44	3.65	4.01	14.22
Total (2013)				10.94	25.7		

[I] Calculated using fresh water discharge (V_q, Table 4) and the DIC concentration of the river water (Table 3).
[II] Calculated using residual flow (V_r, Table 4) and the DIC concentration of the samples collected at the Gangasagar (Table 1).
[III] Calculated using exchange flow (V_x, Table 4) and DIC concentration of the exchange flow (DIC_x) estimated based on Eq. (15). DIC_x was estimated using S_r = salinity at Gangasagar and Freserganj Mohana (Table 1), S_{ocean} = salinity of BoB (Table 3) and $S_{estuary}$ = mean salinity of the samples collected from the estuary in a particular season (Table 1).

degradation of pollutant organic carbon in the Hooghly estuary. The overall effect of anthropogenic sources on the DIC budget of the Hooghly estuary will depend on the nature of the pollutant organic carbon and its rate of degradation, and the residence time of water in the estuary. Studies on the characterization of anthropogenic carbon in these waters are lacking. However, limited experimental studies suggest that up to 80% of the biodegradable fraction of dissolved organic carbon (DOC) could be degraded within 24 h (Seidl et al., 1998, and references therein). Data on effluent waters draining into the Hooghly estuary are not available. However, existing studies indicate that DOC concentrations could be very high in wastewater (25–80 mg/l; Katsoyiannis and Samara, 2006, 2007) and in effluent-dominated rivers (15 mg/l; Duc et al., 2007). These data, together with rapid kinetics of degradation of DOC compared with the residence time of Hooghly River water in the estuary which varies from ca. 10 days to 40 days (Table 4), suggest that carbon sourced from pollution is likely to be degraded during its transport in the estuary. Detailed study of the concentrations and isotopic compositions of DOC in the Hooghly estuary and in the effluent water is needed to quantitatively assess the role of pollution in influencing the cycling of DOC and DIC in the estuary.

5.9. Flux of dissolved inorganic carbon to the Bay of Bengal

Considering that the Hooghly estuary is relatively well mixed (Somayajulu et al., 2002; Ghosh et al., 2013) and that there is very little stratification in the water column in the estuary (Mukhopadhyay et al., 2006), the Land–Ocean Interaction in Coastal Zone (LOICZ) model (Gordon et al., 1996) was used to estimate the annual and seasonal discharge of DIC from the Hooghly River to the BoB. LOICZ model calculations are based on consideration of the mass balance of water, salts and nutrients in coastal systems. These calculations yield results that are essential to assess internal sources or sinks that may play a role in balancing constituent fluxes across the boundary. In this work, a steady-state one-box model was used to calculate the inorganic carbon flux to the BoB. In general, the mass balance of any component y in a single box can be stated as

$$y(t_2) - y(t_1) = \sum \text{Input} - \sum \text{Output} + \Delta y \tag{10}$$

where $y(t)$ signifies the mass of a component in the system at time t; Δy represents the sources and sinks of that component over the specified time interval. $\sum$Input and $\sum$Output represent the sum of all mass fluxes of the component into and out of the system across the boundary.

Water flux from an estuary to the sea is estimated using the following equations

$$V_r = V_q + V_p + V_w + V_0 + V_g - V_e \tag{11}$$

V_q, V_p, V_e, V_w, V_g and V_o represent the volume (per unit time) of river water, precipitation, evaporation, wastewater, groundwater and water from other sources, respectively. The sum of freshwater inflow and outflow from the estuary (evaporation) represents the residual flow (V_r). The seawater exchange flow is expressed by V_x, which is calculated from V_r and salinity (S) as follows:

$$V_x = \frac{V_r S_r}{(S_{ocean} - S_{estuary})} \tag{12}$$

S_r, S_{ocean} and $S_{estuary}$ represent the salinity of the residual flow at the margin of the estuary, salinity of the ocean, and average salinity of the estuary, respectively. All of the data used for the calculations and other details are presented in Table 4.

The residence time of the water in the estuary (τ) is calculated from the equation:

$$\tau = \frac{Vol_{estuary}}{V_r + V_x} \tag{13}$$

where $Vol_{estuary}$ represents the volume of the estuary (8.21×10^9 m^3, Banerjee, 2012). The data used and other details for these calculations are given in Table 4. The results of the LOICZ model calculations for the water budget show that the residence time of water in the estuary varies from ~10 days to ~40 days (Table 4).

Similarly, DIC flux from the estuary is calculated from the following equation:

$$\text{DIC flux} = V_r DIC_r + V_x DIC_x \quad (14)$$

where DIC_r is the DIC concentration at the margin of the estuary, and DIC_x is calculated from the following equation:

$$V_x DIC_x = V_x \left(\frac{DIC_r S_r}{S_{ocean} - S_{estuary}} \right) \quad (15)$$

The addition or removal of inorganic carbon within the estuary can be estimated from the following equation:

$$\text{Addition or removal} = V_r DIC_r + V_x DIC_x - V_q DIC_q \quad (16)$$

The annual DIC flux to the BoB is estimated to be ca. 3.1×10^{11} mol (3.7×10^{12} g) and 2.6×10^{11} mol (3.1×10^{12} g) during the years 2012 and 2013, respectively (Table 5). The inorganic carbon flux is at a maximum during the monsoon season (~60% of the annual value). The calculated DIC fluxes are marginally higher than the DIC flux (2.30×10^{11} mol) reported by Mukhopadhyay et al. (2006). Note that a significant amount of DIC is produced within the Hooghly estuary, accounting for ca. 40–50% of the annual riverine DIC flux to the BoB. The majority of the annual DIC generation (ca. 70%) in the estuary occurs during the monsoon period. Although DIC production over the whole year is a result of a combination of several processes (respiration, organic matter degradation, groundwater contribution), dissolution of carbonate minerals may be the dominant source of additional DIC during the monsoon period, as discussed earlier.

The estimated annual DIC flux from the Hooghly represents ca. 1% of the total DIC flux from the world's rivers to the oceans, which is disproportionately higher than the contribution of water flux from the Hooghly River (ca. 0.2%) to the oceans. Although large rivers such as the Amazon and the Mississippi supply larger amounts of DIC to the oceans annually, a comparison of water and DIC fluxes via large tropical rivers in the world (Table 6) suggests that the ratio of the DIC flux to the water flux is the highest for the Hooghly River. The results of this study emphasize the importance of DIC generation in the Hooghly estuary in supplying disproportionately higher amounts of DIC to the oceans compared with its water flux.

6. CONCLUSIONS

Based on comprehensive data on DIC, $\delta^{13}C_{DIC}$, dissolved Ca and O_2 of the Hooghly estuary over 2 years, the following conclusions can be made: DIC and $\delta^{13}C_{DIC}$ exhibit linear trends with salinity, as expected in a well-mixed estuary, suggesting that mixing accounts for the majority of variability of these parameters. However, variation of DIC and $\delta^{13}C_{DIC}$ cannot be explained only by conservative mixing of river and seawater, particularly in the high salinity zones of the estuary. Mass balance considerations of DIC and $\delta^{13}C_{DIC}$ suggest that the role of biological production and outgassing of CO_2 to the atmosphere are relatively insignificant in influencing the observed variation of DIC and $\delta^{13}C_{DIC}$. In conjunction with data on dissolved O_2, our mixing model calculations suggest that biological respiration and degradation of organic carbon are important ongoing processes in the estuary. A significant amount of DIC is generated within the estuary in the high salinity zone, particularly in the monsoon periods. Based on consideration of mass balance of dissolved Ca in the estuary, we contend that dissolution of carbonate minerals from estuarine and/or marine sediments is the major source of additional DIC in the monsoon period. DIC contributions from anthropogenic activity, estimated to be ca. 2–3% of the river water DIC concentrations, are minor.

LOICZ model calculations indicate that ca. 40–50% of the annual DIC discharge from the Hooghly River to the BoB is generated within the estuary, of which the monsoon period accounts for ca. 70%. This is consistent with the interpretation that a significant amount of DIC is generated by carbonate dissolution during the monsoon period. Every year, ca. $(3–4) \times 10^{12}$ g of DIC is supplied to the Bay of

Table 6
Comparison of DIC contribution from the Hooghly river and other tropical rivers

River	Annual river water discharge (10^{10} m^3)	% Global river water discharge[I]	Annual river DIC flux (10^{12} gm C)	% Global river DIC flux[II]	Ratio of DIC contribution (%) to water supply (%)	Sources of data
Hooghly (Year 2012)	8.3	0.22	3.70	0.94	4.3	This study
Hooghly (Year 2013)	8.3	0.22	3.08	0.81	3.7	This study
Mississippi	57.9	1.5	9.70	2.52	1.7	Wang et al. (2004), Dubois et al. (2010)
Godavari	8.9	0.23	2.27	0.59	2.6	Sarin et al. (2002)
Huanghe	0.8	0.02	0.24	0.06	3.0	Bin and Longjun (2011)
Pearl	31.2	0.89	4.78	1.26	1.4	Guo et al. (2008)
Amazon	750.0	19.70	67.5	17.76	0.9	Druffel et al. (2005), Quay et al. (1992)
Tropical rivers	2520	66.12	210	55.26	0.8	Huang et al. (2012)

[I] Based on global river water flux of 33 to 39 km^3/year Milliman (1991).
[II] Based on global river DIC flux of 0.38×10^{15} g Meybeck (1993).

Bengal via the Hooghly River, which accounts for ca. 1% of the global river DIC flux to the oceans. Comparison with water discharge data indicates that the annual DIC contribution from the Hooghly River (1%) is disproportionately higher than its water supply to the oceans (ca. 0.2%).

This study highlights the importance of internal carbon cycling in a tropical estuary in supplying large amounts of inorganic carbon to the oceans. If such processes of DIC generation are also ongoing in other monsoon dominated estuaries, they could serve as important sources of carbon to the oceans. Our results thus provide an impetus to carry out detailed studies of carbon cycling in other tropical monsoon estuaries.

ACKNOWLEDGEMENTS

SS thanks IISER Kolkata for a research fellowship. This study is funded through a financial grant to TKD by the Ministry of Earth Sciences (MoES), India under the GEOTRACES Program.TKD acknowledges the financial help through the ARF grant from IISER Kolkata. Vikas Agrawal and Prem Chand Kisku are acknowledged for their help during the sampling campaigns. We thank three anonymous reviewers for constructive comments on the manuscript and Dr. Orit Sivan (AE) for editorial handling and useful suggestions.

APPENDIX A.

In this section, we provide brief details on the calculation of Δ[DIC] and $\Delta[\delta^{13}C_{DIC}]$ resulting from degradation of organic carbon, outgassing of CO_2, primary productivity/photosynthesis and carbonate mineral dissolution. These calculations were made following the approach and equations given in Alling et al. (2012).

A.1. Degradation of organic carbon

The $\delta^{13}C$ of DIC subsequent to organic carbon degradation can be expressed as

$$\delta^{13}C_{DIC-F}[DIC]_F = \delta^{13}C_{DIC-I}[DIC]_I + \delta^{13}C_{OC}[DIC]_{OC} \quad (A1)$$

where $\delta^{13}C_{DIC\text{-}I}$ and $[DIC]_I$ are the initial values, prior to degradation of organic carbon, corresponding to $\delta^{13}C_{mix}$ (Eq. (3)) and DIC_{mix} (Eq. (1)). The initial values are based on mixing between freshwater and seawater. $\delta^{13}C_{OC}$ is taken as the average value of $\delta^{13}C_{POC}$ in the Hooghly estuary (−23.7‰; Table 2). $[DIC]_{OC}$ refers to the DIC concentration generated via organic matter degradation. $\delta^{13}C_{DIC\text{-}F}$ and $[DIC]_F$ are the final $\delta^{13}C$ and DIC values resulting from mixing of $[DIC]_I$ and $[DIC]_{OC}$.

The fraction of DIC formed due to degradation of organic carbon (f_{oc}) is given as

$$f_{oc} = \frac{[DIC]_F - [DIC]_I}{[DIC]_F} \quad (A2)$$

Combining Eqs. (A1) and (A2) yields

$$\delta^{13}C_{DIC-F} = f_{oc}(\delta^{13}C_{OC} - \delta^{13}C_{DIC-I}) + \delta^{13}C_{DIC-I} \quad (A3)$$

Using $[DIC]_F$ = measured DIC and $[DIC]_I = DIC_{mix}$ (Eq. (1)), it can be seen that f_{OC} and Δ[DIC] (Eq. (5)) are approximately the same. Thus, Eq. (A3) can be written as:

$$\Delta\delta^{13}C_{DIC} \approx \Delta[DIC](\delta^{13}C_{oc} - \delta^{13}C_{mix}) \quad (A4)$$

Using $\delta^{13}C_{mix} = \delta^{13}C_{DIC}$ of seawater (−0.43‰, Table 3) and river water (−10.7‰, Table 3), the vectors A1 and A2 (Fig. 7) are drawn based on the slopes −23.2 and −12.9, respectively, derived from Eq. (A4). The values for $\delta^{13}C_{mix}$ were chosen to obtain the maximum range in the calculated $\Delta\delta^{13}C_{DIC}$.

A.2. Outgassing of CO_2

Outgassing of CO_2 from water would cause isotopic fractionation between the residual HCO_3^- and CO_2 (aqueous) in the DIC. The fractionation factor (α_{CO_2}), which is temperature dependent, was estimated using the following equation (Rau et al., 1996):

$$\delta^{13}C_{CO_2} = \delta^{13}C_{DIC} + 23.644 - 9701.5/T \quad (A5)$$

where T is the temperature of water in Kelvin and $\delta^{13}C_{DIC}$ is approximately equal to the $\delta^{13}C$ of HCO_3^- in the surface water. The equilibrium fractionation factor (ε_{CO_2}), defined as the difference between $\delta^{13}C_{CO_2}$ and $\delta^{13}C_{DIC}$, was calculated from Eq. (A5) using the average water temperature of 30.1 °C (Table 1). The estimated value of ε_{CO_2} (−8.36) was used to calculate α_{CO_2} based on the following approximation (Emerson and Hedges, 2008):

$$\varepsilon \approx 10^3 \ln\alpha \approx 10^3(\alpha - 1) \quad (A6)$$

This yields a value of 0.992 for α_{CO_2} in the Hooghly estuary waters.

The fraction of DIC remaining in the water (f_{CO_2}) after outgassing of CO_2 is given by:

$$[DIC]_F = f_{CO_2}[DIC]_I \quad (A7)$$

where $[DIC]_I$ is the initial DIC concentration before outgassing (=$[DIC]_{mix}$ calculated based on Eq. (1)), and $[DIC]_F$ is the DIC concentration after CO_2 loss (= measured DIC, Table 1). Due to progressive outgassing of CO_2 by Rayleigh distillation, the resulting $^{13}C/^{12}C$ (R_F) of the Hooghly waters can be determined as follows:

$$R_F = R_I(f_{CO_2})^{\alpha_{CO_2}-1} \quad (A8)$$

where R_I is the initial $^{13}C/^{12}C$ of the water before outgassing (=$(^{13}C/^{12}C)_{mix}$ calculated using $\delta^{13}C_{mix}$ that is derived from Eq. (3)). Using R_F and R_I, the $\delta^{13}C_{DIC\text{-}F}$ of the water can be derived from Eq. (A8) as:

$$\delta^{13}C_{DIC-F} = \delta^{13}C_{DIC-I} + 10^3(\alpha_{CO_2} - 1)\ln(f_{CO_2}) \quad (A9)$$

Due to the small amount of CO_2 subjected to outgassing compared to DIC_{mix}, the $DIC_F/[DIC]_{mix}$ remains close to

1. Combining Eq. (4) with Eqs. (A7) and (A8) yields the following equation:

$$\Delta\delta^{13}C_{DIC} \approx \Delta[DIC]10^3(\alpha_{CO_2} - 1) \quad (A10)$$

This yields a value of −8.36 for the slope of vector B (Fig. 7).

A.3. Primary productivity/Photosynthesis

The fraction of DIC remaining after photosynthetic uptake of carbon (f_{pp}) is given by

$$[DIC]_F = f_{pp}[DIC]_I \quad (A11)$$

where DIC_I refers to concentrations of DIC prior to photosynthesis, and DIC_F refers to the concentrations of DIC remaining after photosynthetic uptake of DIC. Analogous to Eq. (A9), which was derived for outgassing of CO_2, the primary productivity will result in change in the $\delta^{13}C_{DIC}$.

$$\delta^{13}C_{DIC-F} = \delta^{13}C_{DIC-I} + 10^3(\alpha_{pp} - 1)\ln(f_{pp}) \quad (A12)$$

There are two stages of isotopic fractionation during the uptake of carbon via photosynthesis that transfers DIC into the POC pool (Alling et al., 2012). If primary productivity incorporates carbon from CO_2 (aq) with $\delta^{13}C = -8‰$, then using the average $\delta^{13}C_{POC}$ (−23.7‰, Table 2) it can be calculated that the resulting isotope fractionation is −15.63‰. Combining this value with the fractionation associated between CO_2 (aq) and DIC (Eq. (A5)), the total fractionation factor (ε_{pp}) can be computed as −23.99‰. Using this value of ε_{pp}, the fractionation factor (α_{pp}) was estimated to be 0.976.

Using this α value, vector C in Fig. 7 was drawn using the following equation:

$$\Delta\delta^{13}C \approx \Delta[DIC]10^3(\alpha_{pp} - 1) \quad (A13)$$

The slope of the vector C is calculated to be −24.

A.4. Carbonate dissolution

Vectors for carbonate dissolution were drawn in Fig. 7 using the following equation.

$$\Delta\delta^{13}C_{DIC} \approx \Delta[DIC](\delta^{13}C_{carbonate} - \delta^{13}C_{mix}) \quad (A14)$$

This equation was derived following the approach outlined earlier for organic matter degradation. Using $\delta^{13}C_{mix} = \delta^{13}C_{DIC}$ of seawater (−0.43‰, Table 3) and of river water (−10.7‰, Table 3) and $\delta^{13}C_{carbonate} = 0‰$, the slopes of vectors *D*1 and *D*2 were calculated to be 0.43 and 10.72, respectively.

REFERENCES

Abbas N. and Subramanian V. (1984) Erosion and sediment transport in the Ganges river basin (India). *J. Hydrol.* **69**, 173–182.

Abril G., Etcheber H., Delille B., Frankignoulle M. and Borges A. V. (2003) Carbonate dissolution in the turbid and eutrophic Loire estuary. *Marine Ecol. Progress Series.* **259**, 129–138.

Achyuthan H., Deshpande R. D., Rao M. S., Kumar B., Nallathambi T., Shashi Kumar K., Ramesh R., Ramachandran P., Maurya A. S. and Gupta S. K. (2013) Stable isotopes and salinity in the surface waters of the Bay of Bengal: Implications for water dynamics and palaeoclimate. *Mar. Chem.* **149**, 51–62.

Ahad J. M. E., Barth J. A. C., Ganeshram R. S., Spencer R. G. M. and Uher G. (2008) Controls on carbon cycling in two contrasting temperate zone estuaries: The Tyne and Tweed UK. *Estuary Coastal Shelf Sci.* **78**, 685–693.

AHEC. (2011) Assessment of Cumulative impact on Hydropower project in Alakananda and Bhagirathi Basins. 7, 9.

Akhand A., Chandra A., Dutta S. and Hazra S. (2012) Air- water carbon dioxide exchange dynamics along the estuarine transition zone of Sunderban, northern Bay of Bengal, India. *Indian J. Geo-Marine Sci.* **41**, 111–116.

Alling V., Porcelli D., Morth C- M., Anderson L. G., Sanchez-Garcia L., Gustafsson O., Andersson P. S. and Humborg C. (2012) Degradation of terrestrial organic carbon, primary production and out-gassing of CO_2 in the Laptev and East Siberian Seas as inferred from $\delta^{13}C$ values of DIC. *Geochim. Cosmochim. Acta* **95**, 143–159.

Amiotte Suchet P., Probst J.-L. and Ludwig W. (2003) Worldwide distribution of continental rock lithology: Implications for the atmospheric/soil CO_2 uptake by continental weathering and alkalinity river transport to the ocean. *Global Biogeochem. Cycles* **17**(2), 1038.

Aucour A.-M., France-Lanord C., Pedoja K., Pierson-Wickmann A.-C. and Sheppard S. M. F. (2006) Fluxes and sources of particulate organic carbon in the Ganga-Brahmaputra river system. *Global Bogeochem. Cycles.* **20**, GB2006.

Banerjee K. (2012) Biogeochemistry of the Hooghly estuary and adjoining Sunderbans mangrove, India. unpublished Ph. D. thesis. <http://hdl.handle.net/10603/15468>.

Barth J. A. C. and Veizer J. (1999) Carbon cycle in the St. Lawrence aquatic ecosystems at Cornwall (Ontario), Canada: seasonal and spatial variations. *Chem. Geol.* **159**, 107–128.

Basu A. R., Jacobsen S. B., Poreda R. J., Dowling C. B. and Aggarwal P. K. (2001) Large groundwater strontium flux to the oceans from the Bengal Basin and the marine strontium isotope record. *Science* **293**, 1470.

Battin T. J., Luyssaert S., Kaplan L. A., Aufdenkampe A. K., Richter A. and Tranvik L. J. (2009) The boundless carbon cycle. *Nat. Geosci.* **2**, 598–600.

Bauer J. E., Cai W.-J., Raymond P. A., Bianchi T. S., Hopkinson C. S. and Regnier P. A. G. (2013) The changing carbon cycle of the coastal ocean. *Nature* **504**, 61–70.

Bin X. and Longjun Z. (2011) Carbon distribution and fluxes of 16 rivers discharging into the Bohai Sea in summer. *Octanol Acta.* **30**, 43–54.

Biswas H., Mukhopadhyay S. K., Sen S. and Jana T. K. (2007) Spatial and temporal pattern of methane dynamics in the tropical mangrove dominated estuary, NE coast of Bay of Bengal, India. *J. Marine Sci.* **68**, 55–64.

Bouillon S., Frankignoulle M., Dehairs F., Velimirov B., Eiler A., Abril G., Etcheber H. and Borges A. V. (2003) Inorganic and organic carbon biogeochemistry in the Gautami Godavari estuary (Andhra Pradesh, India) during pre-monsoon: the local impact of extensive mangrove forests. *Global Biogeochem. Cycles* **17**(4), 1114.

Brunet F., Gaiero D., Probst J. L., Depetris P. J., Gauthier Lafaye F. and Stille P. (2005) $\Delta^{13}C$ tracing of dissolved inorganic carbon sources in Patagonian rivers (Argentina). *Hydrol. Process.* **19**, 3321–3344.

Cai W.-J. and Wang Y. (1998) The chemistry, fluxes and sources of carbon dioxide in estuarine waters of the Satilla and Altamaha Rivers, Georgia. *Limnol. Oceanogr.* **43**(4), 657–668.

Chanton J. P. and Lewis F. G. (1999) Plankton and dissolved inorganic carbon isotopic composition in river-dominated Estuary: Apalachicola Bay, Florida. *Estuaries* **22**, 575–583.

Choudhury A. K. and Pal R. (2012) Understanding the seasonal dynamics of primary productivity in relation to phytoplankton populations from the Bhagirathi – Hooghly estuary, eastern Indian coast. *J. Algal Biomass Utln.* **3**(4), 80–88.

CIFRI (2012) Present status of Hilsa in Hooghly – Bhagirathi river. Central Inland Fisheries Research Institute. <www.cifri.ernet.in/179.pdf>.

Cole J. J., Prairie Y. T., Caraco N. F., McDowell W. H., Tranvik L. J., Striegl R. G., Duarte C. M., Kortelainen P., Downing J. A., Middelburg J. J. and Melack J. (2007) Plumbing the global carbon cycle: integrating inland waters into the terrestrial carbon budget. *Ecosystems* **10**, 171–184.

Dalai T. K., Krishnaswami S. and Sarin M. M. (2002a) Major ion chemistry in the headwaters of the Yamuna river system: chemical weathering, its temperature dependence and CO_2 consumption in the Himalaya. *Geochim. Cosmochim. Acta* **66**, 3397–3416.

Dalai T. K., Krishnaswami S. and Sarin M. M. (2002b) Barium in the Yamuna River system in the Himalaya: sources, fluxes and its behavior during weathering and transport. *Geochem. Geophys. Geosyst.* **3**. http://dx.doi.org/10.1029/2002GC000381.

Dalai T. K., Singh S. K., Trivedi J. R. and Krishnaswami S. (2002c) Dissolved Rhenium in the Yamuna River System and the Ganga in the Himalaya: Role of black shale weathering on the budgets of Re, Os, and U in rivers and CO_2 in the atmosphere. *Geochim. Cosmochim. Acta* **66**, 29–43.

De T. K., Ghosh S. K., Jana T. K. and Choudhoury A. (1991) Phytoplankton bloom in the Hooghly Estuary. *Indian J. Marine Sci.* **20**, 134–137.

de Jonge V. N. and Viilerius L. A. (1989) Possible role of carbonate dissolution in estuarine phosphate dynamics. *Limnol. Oceanogr.* **34**, 332–340.

Doctor D. H., Kendall C., Sebestyen D., Shanley J. B., Ohte N. and Boyer E. W. (2008) Carbon isotope fractionation of dissolved inorganic carbon(DIC) due to outgassing of carbon dioxide from ahead water stream. *Hydrol. Process.* **22**, 2410–2423.

Dowling C. B., Poreda R. J. and Basu A. R. (2003) The groundwater geochemistry of the Bengal Basin: Weathering, chemsorption, and trace metal flux to the oceans. *Geochim. Cosmochim. Acta* **67**, 2117–2136.

Druffel E. R. M., BauerJ E. and Griffin S. (2005) Input of particulate organic and dissolved inorganic carbon from the Amazon to the Atlantic Ocean. *Geochem. Geophys. Geosyst.* **6**, Q03009.

Dubois K. D., Lee D. and Veizer J. (2010) Isotopic constraints on alkalinity, dissolved organic carbon and atmospheric carbon dioxide fluxes in the Mississippi River. *J. Geophys. Res.* **115**, 2–11.

Duc T. A., Vachaud G., Bonnet M. P., Prieur N., Loi V. D. and Anh L. L. (2007) Experimental investigation and modelling approach of the impact of urban wastewater on a tropical river; a case study of the Nhue River, Hanoi, Viet Nam. *J. Hydrol.* **334**, 347–358.

Dutta K., Ravi Prasad G. V., Ray D. K. and Raghav K. (2010) Decadal changes of Radiocarbon in the surface Bay of Bengal: Three decades after GEOSECS and one decade after WOCE. *Radiocarbon* **52**(2–3), 1191–1196.

Dutta M. K., Mukherjee R., Jana T. K. and Mukhopadhyay S. K. (2015) Biogeochemical dynamics of exogenous methane in an estuary associated to a mangrove biosphere; The Sundarbans, NE coast of India. *Marine Chem.* **170**, 1–10.

Emerson S. R. and Hedges J. I. (2008) Chemical Oceanography and the Marine Carbon Cycle.Cambridge University Press, New York. 1, 464.

Fearnside P. M. (2000) Global warming and tropical land-use change: Greenhouse gas emissions from biomass burning, decomposition and soils in forest conversion, shifting cultivation and secondary vegetation. *Clim. Change* **46**(1–2), 115–158.

Fontugne M. R. and Duplessy J.-C. (1981) Organic carbon isotopic fractionation by marine plankton in the temperature range −1 to 31 °C. *Oceanol. Acta* **4**, 85–90.

Ghosh P., Chakrabarti R. and Bhattacharya S. K. (2013) Short- and long-term temporal variations in salinity and the oxygen, carbon and hydrogen isotopic compositions of the Hooghly Estuary water, India. *Chem. Geol.* **335**, 118–127.

Gordon, Jr., D. C., Boudreau P. R., Mann K. H., Ong J- E., Silvert W. L., Smith S. V., Wattayakorn G., Wulff F. and Yanagi T. (1996) LOICZ Biogeochemical Modeling Guidelines. *LOICZ Rep. Studies* **5**, 1–96.

Guo X., Cai W.-J., Zhai W., Dai M., Wang Y. and Chen B. (2008) Seasonal variations in the inorganic carbon system in the Pearl River (Zhujiang) estuary. *Cont. Shelf Res.* **28**, 1424–1434.

Guzzella L., Roscioli C., Vigano L. M., Saha M., Sarkar S. K. and Bhattacharya A. (2005) Evaluation of the concentration of HCH, DDT, HCB, PCB and PAH in the sediments along the lower stretch of Hugli estuary, West Bengal, northeast India. *Environ. Int.* **31**, 523–534.

Hélie J-F., Hillaire- Marcel C. and Rondeau B. (2002) Seasonal changes in the sources and f luxes of dissolved inorganic carbon through the St Lawrence River—isotopic and chemical constraint. *Chem. Geol.* **186**, 117–138.

Hellings L., Dehairs F., Tackx M., Keepens E. and Baeyens W. (1999) Origin and fate of organic carbon in the freshwater part of Scheldt estuary as traced by stable carbon isotope composition. *Biogeochemistry* **47**, 167–186.

Huang T.-H., Fu Y.-H., Pan P.-Y. and Arthur Chen C.-T. (2012) Fluvial carbon fluxes in tropical rivers. *Curr. Opin. Environ. Sustain.* **4**, 162–169.

Hunt E. R., Piper S. C., Nemani R., Keeling C. D., Otto R. D. and Running S. W. (1996) Global net carbon exchange and intra-annual atmospheric CO_2 concentrations predicted by an ecosystem process model and three dimensional atmospheric transport model. *Global Biogeochem. Cycles* **10**, 431–456.

IMD (2013)District wise (South 24 Parganas) rainfall data for last five years. Indian Meteorological Department. <www.imd.gov.in/section/hydro/distrainfall/webrain/wb/south24parganas.txt>.

Ittekkot V., Safiullah S., Mycke B. and Seifert R. (1985) Seasonal variability and geochemical significance of organic matter in the river Ganga, Bangladesh. *Nature* **317**, 800–802.

Katsoyiannis A. and Samara C. (2006) Ecotoxicological evaluation of the wastewater treatment process of the sewage treatment plant of Thessaloniki, Greece. *J. Hazard. Mater.* **141**, 614–621.

Katsoyiannis A. and Samara C. (2007) The Fate of Dissolved Organic Carbon (DOC) in the wastewater treatment process and its importance in the removal of wastewater contaminants. *Environ. Sci. Pollut. Res.* **14**, 284–292.

Keeling C. D., Mook W. G. and Tans P. P. (1979) Recent trends in the ^{13}C–^{12}C ratio of atmospheric carbon- dioxide. *Nature* **277**, 121–123.

Keeling C. D., Bacastow R. B. and Tans P. P. (1980) Predicted shift in the ^{13}C–^{12}C ratio of atmospheric carbon-dioxide. *Geophys. Res. Lett.* **7**, 505–508.

Mandal S., Debnath M., Ray S., Ghosh P. B., Roy M. and Ray S. (2012) Dynamic modelling of dissolved oxygen in the creeks of Sagar island, Hooghly-Matla estuarine system, West Bengal, India. *Appl. Mathemat. Model.* **36**, 5952–5963.

Meybeck M. (1993) C, N, P and S in rivers: from sources to global inputs. In *Interaction of C, N, P and S Biogeochemical Cycles and Global Change* (eds. R. Wollast, F. T. Mackenzie and L. Chou). Springer Verlag, pp. 163–193.

Milliman J. D. (1991) The flux and fate of fluvial sediment and water in coastal seas. In *Ocean Margin Processes in Global Change* (eds. R. F. C. Mantoura, J. -M. Martin and R. Wollast). John Wiley and Sons Ltd. pp. 69–89.

Milliman J. D. and Meade R. H. (1983) World-wide delivery of river sediment to the oceans. *J. Geol.* **91**, 1–21.

Mook W. G. and Koene B. K. S. (1975) Chemistry of dissolved inorganic carbon in estuarine and coastal brackish waters. *Estuar. Coast. Mar. Sci.* **3**, 325–336.

Mook W. G. and Tan T. C. (1991) Stable carbon isotopes in rivers and estuaries. In *Biogeochemistry of Major World Rivers* (eds. E. T. Degens, S. Kempe and J. E. Richey). SCOPE, John Wiley and Sons Ltd, pp. 245–264.

Moore W. S. (1997) High fluxes of radium and barium from the mouth of the Ganges-Brahmaputra River during low river discharge suggest large groundwater source. *Earth Planet. Sci. Lett.* **150**, 141–150.

Mucci A. (1983) The solubility of calcite and aragonite in seawater at various salinities, temperatures, and one atmosphere total pressure. *Am. J. Sci.* **283**, 780–799.

Mukhopadhyay S. K., Biswas H., De T. K., Sen S. and Jana T. K. (2002) Seasonal effects on the air–water carbon dioxide exchange in the Hooghly estuary, NE coast of Bay of Bengal, India. *J. Environ. Monitor.* **4**, 549–552.

Mukhopadhyay S. K., Biswas H., De T. K. and Jana T. K. (2006) Fluxes of nutrients from the tropical River Hooghly at the land–ocean boundary of Sundarbans, NE Coast of Bay of Bengal, India. *J. Marine Syst.* **62**, 9–21.

Quay P. D., Wilbur D. O., Richey J. E., Hedges J. I. and Devol A. H. (1992) Carbon cycling in the Amazon River: Implication from the ^{13}C composition of particles and solutes. *Limnol. Oceanogr.* **37**, 857–871.

Rai S. K., Singh S. K. and Krishnaswami S. (2010) Chemical weathering in the plain and peninsular sub-basins of the Ganga: impact on major ion chemistry and elemental fluxes. *Geochim. Cosmochim. Acta* **74**, 2340–2355.

Rau G. H., Riebesell U. and Wolf-Gladrow D. (1996) A model of photosynthetic C-13 fractionation by marine phytoplankton based on diffusive molecular CO_2 uptake. *Mar. Ecol. Prog. Ser.* **133**, 275–285.

Regnier P., Friedlingstein P., Ciais P., Mackenzie F. T., Gruber N., Janssens I. A., Laruelle1 G. G., Lauerwald R., Luyssaert S., Andersson A. J., Arndt S., Arnosti C., Borges A. V., Dale A. W., Gallego-Sala A., Goddéris Y., Goossens N., Hartmann J., Heinze C., Ilyina T., Joos F., LaRowe D. E., Leifeld J., Meysman R. F. J., Munhoven G., Raymond P. A., Spahni R., Suntharalingam P. and Thullner M. (2013) Anthropogenic perturbation of the carbon fluxes from land to ocean. *Nat. Geosci.* **6**, 597–607.

Richey J. E., Melack J. M., Aufdenkampe A. K., Ballester V. M. and Hess L. L. (2002) Outgassing from Amazonian rivers and wetlands as a large tropical source of atmospheric CO_2. *Nature* **416**, 617–620.

Rodelli M. R., Gearing J. N., Gearing P. J., Marshall N. and Sasekumar A. (1984) Stable isotope ratio as a tracer of mangrovecarbon in Malaysian ecosystem. *Oecologia* **61**, 326–333.

Romanek C. S., Grossman E. L. and Morse J. W. (1992) Carbon isotopic fractionation in synthetic aragonite and calcite: effects of temperature and precipitation rate. *Geochim. Cosmochim. Acta* **56**, 419–430.

Rudra K. (2014) Changing river courses in the western part of the Ganga-Brahmaputra delta. *Geomorphology* **227**, 87–100.

Sabine C. L., Key R. M., Feely R. A. and Greeley D. (2002) Inorganic carbon in the Indian Ocean: distribution and dissolution processes. *Global Biogeochem. Cycles* **16**(4), 1067.

Sadhuram Y., Sarma V. V., Ramana Murthy T. V. and Prabhakara Rao B. (2005) Seasonal variability of physico-chemical characteristics of Haldia channel of Hooghly estuary, India. *J. Earth Syst. Sci.* **114**, 37–49.

Sarin M. M., Krishnaswami S., Dilli K., Somayajulu B. L. K. and Moore W. S. (1989) Major ion chemistry of the Ganga-Brahmaputra river system weathering processes and fluxes to the Bay of Bengal. *Geochim. Cosmochim. Acta* **53**, 997–1009.

Sarin M., Sudheer A. K. and Balakrishna K. (2002) Significance of riverine carbon transport: A case study of a large tropical river, Godavari (India). *Sci. China.* **45**, 98–108.

Sarma V. V. S. S., Krishna M. S., Rao V. D., Viswanadham R., Kumar N. A., Kumari T. R., Gawade L., Ghatkar S. and Tari A. (2012) Sources and sinks of CO_2 in the west coast of Bay of Bengal. *Tellus B.* **64**, 10961.

Schulte P., van Geldern R., Freitag H., Karim A., Négrel P., Petelet-Giraud E., Probst A., Probst J.-L., Telmer K., Veizer J. and Barth J. A. C. (2011) Applications of stable water and carbon isotopes in watershed research: weathering, carbon cycling, and water balances. *Earth Sci. Rev.* **109**, 20–31.

Seidl M., Servais P. and Mouchel J. M. (1998) Organic matter transport and degradation in the river Seine (France) after a combined sewer overflow. *Water Res.* **32**, 3569–3580.

Sen Gupta R., Naik S. and Singbal S. Y. S. (1978) A study of fluoride, calcium and magnesium in the Northern Indian Ocean. *Mar. Chem.* **6**, 125–141.

Singh S. K., Trivedi J. R., Pande K., Ramesh R. and Krishnaswami S. (1998) Chemical and Sr, O, C isotopic compositions of carbonates from the Lesser Himalaya: implications to the Sr isotope composition of the source waters of the Ganga, Ghaghara and the Indus Rivers. *Geochim. Cosmochim. Acta* **62**, 743–755.

Singh S. K., Rai S. K. and Krishnaswami S. (2008) Sr and Nd isotopes in river sediments from the Ganga basin: sediment provenance and hotspots of physical erosion. *J. Geophys. Res.* **113**, F03006.

Sinha P. C., Guliani P., Jena G. K., Rao A. D., Dube S. K., Chatterjee A. K. and Murty T. (2004) A breadth averaged numerical model for suspended sediment transport in Hooghly estuary, East Coast of India. *Nat. Hazard.* **32**, 239–255.

Somayajulu B. L. K., Rengarajan R. and Jani R. A. (2002) Geochemical cycling in the Hooghly estuary, India. *Marine Chem.* **79**, 171–183.

Unger D., Ittekkot V., Schafer P., Tiemann J. and Reschke S. (2003) Seasonality and interannual variability of particle fluxes to the deep Bay of Bengal: influence of riverine input and oceanographic processes. *Deep Sea Res. II.* **50**, 897–923.

van Geldern R., Schulte P., Mader M., Baier A. and Barth J. A. C. (2015) Spatial and temporal variations of pCO_2, dissolved inorganic carbon and stable isotopes along a temperate karstic watercourse. *Hydrol. Process.*. http://dx.doi.org/10.1002/hyp.10457.

Wang X.-C., Chen R. F. and Gardner G. B. (2004) Sources and transport of dissolved and particulate organic carbon in the Mississippi River estuary and adjacent coastal waters of the northern Gulf of Mexico. *Mar. Chem.* **89**, 241–256.

Weiss R. F. (1974) Carbon dioxide in water and seawater: the solubility of a non-ideal gas. *Mar. Chem.* **2**, 203–215.

Whiticar M. J. and Faber E. (1986) Methane oxidation in sediment and water column environments-Isotope evidence. *Org. Geochem.* **10**, 759–768.

Yao G., Gao Q., Wang Z., Huang X., He T., Zhang Y., Jiao S. and Ding J. (2007) Dynamics of CO_2 partial pressure and CO_2 outgassing in the lower reaches of the Xijiang River, a subtropical monsoon river in China. *Sci. Total Environ.* **376**, 255–266.

Zhai W., Dai M., Cai W.-J., Wang Y. and Wang Z. (2005) High partial pressure of CO_2 and its maintaining mechanism in a subtropical estuary: the Pearl River estuary, China. *Marine Chem.* **93**, 21–32.

Associate editor: Orit Sivan